ENGINEERING RESEARCH INSTITUTE
THE UNIVERSITY OF MICHIGAN
ANN ARBOR

Final Report

THEORETICAL TOSS-BOMBING STUDY

George E. Hay
Edward Young

Project 1699-1

DEPARTMENT OF THE AIR FORCE
WRIGHT AIR DEVELOPMENT CENTER
WRIGHT-PATTERSON AIR FORCE BASE, OHIO
CONTRACT NO. W33(038)ac-15318
PROJECT NO. 54-650A-460

September 1955

TABLE OF CONTENTS

ABSTRACT

An airplane approaches a target T at a constant speed V along a straight line which makes an angle ϵ with the horizontal. When the airplane is at a distance R_o from the target, it pulls up in a 3g turn through an angle θ while maintaining its constant speed V. The airplane then releases a bomb which travels a ballistic trajectory and bursts on the target. The purpose of this study is the preparation of a number of graphs from which pertinent information regarding the various bombing runs can be read. In particular, Fig. 2 readily yields the values of ϵ, the time of flight of the bomb, and the minimum ground clearance for a general bombing run identified by the values of R_o and θ associated with it. Also, Fig. 4 accomplishes the same purpose when the bombing run is identified by the rectangular cartesian coordinates of the airplane at the instant when the pull-up begins; Fig. 5 is the same as Fig. 4, except that the bombing run is identified by the rectangular cartesian coordinates of the airplane at the instant when the bomb is released. Figures 6-9 in a similar fashion yield the values of five error coefficients associated with a general bombing run. These error coefficients permit the calculation of the maximum amounts by which the burst misses the target due to small errors in ϵ, R_o, and θ, and in the prescribed 3g pull-up. Figures 12-14 show some typical bombing runs.

OBJECTIVE

This report is devoted to an analysis leading to the construction of various graphs containing information pertinent to toss bombing.

LIST OF NOTATIONS

ϵ: angle of approach. See Fig. 1.

V: velocity of the airplane.

g: acceleration due to gravity.

n: pull-up constant. The airplane pulls up into an ng turn.

R_o: range at pull-up beginning. See Fig. 1.

θ: pull-up angle. See Fig. 1.

q: minimum ground clearance. See Fig. 3.

r: radius of the pull-up circle. See Fig. 1.

t: the time, measured from the instant of bomb release.

(x, y): coordinates of the bomb at time t.

(x_B, y_B): (x, y) at the time of burst.

L': a standard length $= V^2/g$.

T': a standard time $= V/g$.

τ: the modified time $= t/T'$.

Q: the modified minimum ground clearance $= q/L'$.

ρ: the modified range $= R_o/L'$.

(λ, μ): modified coordinates of the bomb $= (x/L', y/L')$.

(ξ, ζ): $(x/R_o, y/R_o)$. See Equations (3.4).

(ξ_B, ζ_B): (ξ, ζ) at the time of burst.

T: value of τ at the time of burst.

ρ_{max}: maximum value of ρ for given ϵ.

Φ: defined in Equation (6.2).

Ψ: defined in Equation (6.3).

ϕ: defined in Equation (8.5).

ψ: defined in Equation (8.6).

$\bar{\phi}$: defined in Equation (14.3).

$\bar{\psi}$: defined in Equation (14.3).

$\delta\theta$, δR, $\delta\epsilon$, δn: errors in θ, R, ϵ, n, respectively.

δx_B, δy_B: horizontal and vertical errors in the location of the burst. See Section 24, par. 2.

α: angle of inclination of the trajectory in the neighborhood of the target.

E_x, E_y, E_θ, E_R, E_ϵ, E_n: percent errors defined in Equations (24.2).

$E_{x\theta}$, $E_{y\theta}$, $E_{\theta R}$, $E_{\theta\epsilon}$, $E_{\theta n}$: error coefficients defined in Equations (26.9).

SECTION 1: INTRODUCTION

The reader who is concerned only with the results of this study, and not with the theory on which these results are based, may skip Sections 6-9, 12-16, 19-23, and 26.

An airplane approaches a target T along a straight line AOT which makes an angle ϵ with the horizontal, as illustrated in Fig. 1. At O the airplane pulls up onto a circular path OR. At R a bomb is released which follows a ballistic path and bursts at a point B. The speed of the airplane over its entire path is a constant V. The radial acceleration of the airplane on the circular path OR is thus a constant which will be denoted by ng, where g is the acceleration due to gravity and n is a dimensionless constant called the pull-up constant. We shall be particularly concerned with the case $n = 3$, but in order to make a determination of the effect of small variations in n away from 3, we shall leave n unspecified for the present.

The slant range of the airplane from the target when the pull-up begins is R_o, and the pull-up angle when the bomb is released is θ, as shown in Fig. 1. In this study it is proposed to prepare several families of curves which present in a compact form pertinent information regarding the various bombing runs culminating in a bomb burst on the target. These curves are such as to permit one to read off at a glance, for any trajectory, the values of the slant range R_o, the angle of approach ϵ, the pull-up angle θ, the time of free flight of the bomb, the minimum ground clearance q, the coordinates of the pull-up point O, and the coordinates of the point R where the bomb is released. It is also proposed to present curves showing the amounts by which the burst might miss the target in both elevation and range due to small errors in the pull-up angle θ, the slant range R_o, the angle of approach ϵ, and the pull-up constant n.

Actually, these curves will be expressed, not in terms of the quantities defined above, but in terms of certain equivalent dimensionless quantities to be defined in the next section. The various curves appear in Figs. 2 and 4-9. The precise description of the meanings of these curves is quite involved. As may be seen from the Table of Contents, the explanations of these figures appear in Sections 4, 10, 17, and 24. The Table of Contents also indicates where the theory pertaining to the curve families appearing in these figures may be found.

SECTION 2: THE EQUATIONS OF MOTION

We refer here to Fig. 1. As stated in Section 1, the airplane travels the circular arc OR at a constant speed V and a radial acceleration ng. If r is the radius of this circular path, then we have $V^2/r = ng$, so that

$$r = V^2/ng. \tag{2.1}$$

The lines TO, OE and ER, with the positive x-axis, make the angles ϵ, $\epsilon + (1/2)\pi$, and $\epsilon + (1/2)\pi + (\pi - \theta)$, respectively. Thus, by projecting the broken line TOER on the x- and y-axes, we find that the coordinates of R are $[R_o \cos \epsilon + r \cos\{(1/2)\pi + \epsilon\} + r \cos\{(3/2)\pi + \epsilon - \theta\}$, $R_o \sin \epsilon + r \sin\{(1/2)\pi + \epsilon\} + r \sin\{(3/2)\pi + \epsilon - \theta\}]$, or

$$[R_o \cos \epsilon - r \sin \epsilon + r \sin (\epsilon - \theta), R_o \sin \epsilon + r \cos \epsilon - r \cos (\epsilon - \theta)]. \tag{2.2}$$

The velocity of the bomb at R makes an angle with the position x-axis of $\epsilon + \pi - \theta$. Thus, the velocity components of the bomb at this instant are $[V \cos (\pi + \epsilon - \theta), V \sin (\pi + \epsilon - \theta)]$, or

$$[- V \cos (\epsilon - \theta), - V \sin (\epsilon - \theta)]. \tag{2.3}$$

Let t denote the time of flight of the bomb, measured from the instant when the bomb is released, and let (x,y) denote the coordinates of the bomb at time t. From (2.2) and (2.3) it then follows that

$$\left.\begin{aligned} x &= R_o \cos \epsilon - r \sin \epsilon + r \sin (\epsilon - \theta) - Vt \cos (\epsilon - \theta), \\ y &= R_o \sin \epsilon + r \cos \epsilon - r \cos (\epsilon - \theta) - Vt \sin (\epsilon - \theta) - \tfrac{1}{2} gt^2. \end{aligned}\right\} \tag{2.4}$$

These are the equations of motion of the bomb.

SECTION 3: DIMENSIONLESS QUANTITIES

THE FUNDAMENTAL EQUATIONS

The desired results in this study can be expressed more compactly in terms of dimensionless quantities rather than in terms of those introduced heretofore. To this end we introduce a standard length L' and a standard time T' which we define by the relations

$$L' = V^2/g, \quad T' = V/g. \tag{3.1}$$

It will be noted that L' is the radius of a 1g turn made at speed V. If, for example, V is equal to Mach 1, then L' is equal to approximately 30,000 ft, and T is equal to approximately 30 sec.

We now introduce a dimensionless time τ and a dimensionless slant range ρ defined by

$$\tau = t/T', \quad \rho = R_o/L'. \tag{3.2}$$

We also introduce dimensionless coordinates (λ, μ) defined by

$$\lambda = x/L', \quad \mu = y/L'. \tag{3.3}$$

The quantities τ, ρ, λ, and μ will be referred to as the modified time, modified range, and modified coordinates, respectively. We shall also find it convenient to introduce a second set of dimensionless quantities (ξ, ζ) defined by

$$\xi = x/R_o, \quad \zeta = y/R_o. \tag{3.4}$$

Let us now express the equations of motion (2.4) in terms of dimensionless quantities. We substitute in (2.4) for t, R_o, x, y from (3.2) and (3.3), and also substitute for r from (2.1) to obtain the modified equations of motion,

$$\left.\begin{aligned} \rho(\xi - \cos\epsilon) + \frac{1}{n}[\sin\epsilon - \sin(\epsilon - \theta)] + \tau\cos(\epsilon - \theta) &= 0, \\ \rho(\zeta - \sin\epsilon) - \frac{1}{n}[\cos\epsilon - \cos(\epsilon - \theta)] + \tau\sin(\epsilon - \theta) + \frac{1}{2}\tau^2 &= 0. \end{aligned}\right\} \quad (3.5)$$

The bomb bursts at the point B, which may or may not coincide with the target. Let us suppose that the burst occurs at a modified time $\tau = T$, the corresponding values of (ξ, ζ) being (ξ_B, ζ_B). Then (3.5) yields

$$\rho(\xi_B - \cos\epsilon) + \frac{1}{n}[\sin\epsilon - \sin(\epsilon - \theta)] + T\cos(\epsilon - \theta) = 0, \quad (3.6)$$

$$\rho(\zeta_B - \sin\epsilon) - \frac{1}{n}[\cos\epsilon - \cos(\epsilon - \theta)] + T\sin(\epsilon - \theta) + \frac{1}{2}T^2 = 0. \quad (3.7)$$

These equations are fundamental in the developments which follow and will be referred to as the fundamental equations.

SECTION 4: FIGURE 2

EXPLANATIONS

Figure 2 presents in convenient form information concerning the various bombing runs specified by assigned values of the modified slant range ρ and the pull-up angle θ. This statement is amplified below. This figure deals with a situation in which the bomb bursts on the target, and the pull-up constant n has the value 3, so that the airplane pulls up into a 3g turn. It is intuitively obvious that in such a situation the assignment of values of ϵ and ρ completely specifies a bombing run. We may then regard θ as a function of ϵ and ρ, and write

$$\theta = \theta(\epsilon, \rho). \quad (4.1)$$

Of course, there are bounds placed on the values assigned to ϵ and ρ, because of physical limitations. Equivalently, we may specify a bombing run by the assignment of values to ρ and θ. In Fig. 2, ρ is plotted horizontally and θ is plotted vertically. It thus appears that, to each point in some region in the (ρ, θ) plane of Fig. 2, there corresponds a bombing run, and vice versa.

In Fig. 2 there are three families of curves and a single curve besides. These will now be explained in turn.

The Family ϵ = Const.—As mentioned above, to each bombing run there corresponds a point in the (ρ, θ) plane of Fig. 2. The curves ϵ = const. in Fig. 2 indicate the values of the angle of approach ϵ associated with the various bombing runs. The theory leading to the determination of the curves of this family is developed in Section 6.

The Curve $\rho = \rho_{max}$.—To each bombing run there corresponds a point in the (ρ, θ) plane of Fig. 2. The points on the curve $\rho = \rho_{max}$ correspond to bombing runs for which ϵ is assigned and ρ is as large as possible. It will be noted that this curve cuts each curve of the family ϵ = const. where ρ is as large as possible, as might be expected. The theory leading to the determination of the curve $\rho = \rho_{max}$ is developed in Section 7.

The Family T = Const.—It will be recalled that T is the modified time of free flight of the bomb. To each bombing run there corresponds a point in the (ρ, θ) plane of Fig. 2. The curves T = const. in Fig. 2 indicate the values of T associated with the various bombing runs. The theory leading to the determination of the curves of this family is developed in Section 8.

The Family Q = Const.—It is assumed that the surface of the ground is a horizontal plane containing the x-axis of Fig. 1. The minimum ground clearance of the airplane, which occurs at a point on the pull-up circle, will be denoted by q. We introduce a corresponding dimensionless quantity Q defined by the relation

$$Q = q/L', \tag{4.2}$$

where L' is the standard length defined in Section 3.

To each bombing run there corresponds a point in the (ρ, θ) plane of Fig. 2. The curves Q = const. in Fig. 2 indicate the values of Q associated with the various bombing runs. The theory leading to the determination of the curves of this family is developed in Section 9.

SECTION 5: FIGURE 2

EXAMPLES OF ITS USE

Example 1.—Let us suppose an airplane approaches the target at 1000 ft/sec^{-1} with an angle of approach of 30°, and starts the pull-up at a range of 60,000 ft. Then V = 1000, ϵ = 30°, and R_0 = 60,000. For convenience we take g = 32 ft/sec^{-2}. Then the standard length L' and the stan-

dard time T' have the values $L' = V^2/g = 10^6/32 = 31{,}250$ ft and $T' = V/g = 1000/32 = 31.250$ sec. Then $\rho = R_o/L' = 1.92$, and the point A in Fig. 2 corresponds to the bombing run under consideration here. From Fig. 2 it then follows that $\theta = 36.2°$ and, by the use of linear interpolation on the families of curves T = const. and Q = const., that T = 1.47 and Q = 0.92. The time of free flight of the bomb is $TT' = 1.47 \times 31.250 = 45.9$ sec, and the minimum ground clearance of the airplane is $QL' = 0.92 \times 31{,}250 = 29 \times 10^3$ ft.

Example 2.—An airplane approaches the target at 1000 ft/sec^{-1} with an angle of approach of 30°. It is desired to investigate the bombing run for which the slant range at the instant of pull-up beginning is as large as possible. As in Example 1, we have V = 1000 and $\epsilon = 30°$, and for convenience we take g = 32 ft/sec^{-2}, and so $L' = 31{,}250$ ft and $T' = 31.250$ sec. The point B in Fig. 2 corresponds to the bombing run under consideration. From Fig. 2 it then follows that $\rho = 2.58$ and $\theta = 64.2°$. The range at which the pull-up begins is thus $R_o = \rho L' = 2.58 \times 31{,}250 = 806 \times 100$ ft. As in Example 1, linear interpolation yields T = 2.27 and Q = 1.24. Thus, the time of free flight of the bomb is $TT' = 2.27 \times 31.25 = 70.9$ sec, and the minimum ground clearance of the airplane is $QL' = 1.24 \times 31{,}250 = 38.8 \times 1000$ ft.

SECTION 6: FIGURE 2

THEORY FOR THE CURVE FAMILY ϵ = CONST.

The determination of this curve family is based on the fundamental equations (3.6) and (3.7). Now Fig. 2 refers to bombing runs for which the bomb bursts on the target, so in (3.6) and (3.7) we should set $\xi_B = \zeta_B = 0$. However, for later convenience we shall defer this step temporarily.

It will be recalled that in the present study the pull-up constant n has the value 3. Thus (3.6) and (3.7) are two equations involving the parameters ρ, ϵ, θ, and T. Let us eliminate T between these two equations. We readily solve (3.6) for T and then substitute in (3.7). This yields an equation quadratic in ρ. After some simplification, this equation takes the form

$$\rho^2 - 2\Phi\rho + \Psi = 0, \qquad (6.1)$$

where

$$\Phi = \frac{1}{2(\xi_B - \cos\epsilon)}\left\{\sin 2(\epsilon - \theta) - \frac{\zeta_B - \sin\epsilon}{\xi_B - \cos\epsilon}[1 + \cos 2(\epsilon - \theta)] - \frac{2}{n}[\sin\epsilon - \sin(\epsilon - \theta)]\right\}, \tag{6.2}$$

$$\Psi = \frac{1}{n(\xi_B - \cos\epsilon)^2}\left\{2(1 - \cos\theta)\cos(\epsilon - \theta) + \frac{1}{n}[\sin\epsilon - \sin(\epsilon - \theta)]^2\right\}. \tag{6.3}$$

Solving (6.1) for ρ, we obtain

$$\rho = \Phi \pm \sqrt{\Phi^2 - \Psi}\,. \tag{6.4}$$

Referring to Fig. 1, we note that the lower sign in (6.4) gives a smaller value of ρ than does the upper sign. This smaller value corresponds to the case where the bomb leaves the release point R with a speed V downward along the parabola. This case is extraneous. Hence, we have

$$\rho = \Phi + \sqrt{\Phi^2 - \Psi}. \tag{6.5}$$

When the bomb bursts on the target, we have $\xi_B = \zeta_B = 0$, so that

$$\Phi = -\frac{1}{2\cos\epsilon}\left\{\sin 2(\epsilon - \theta) - \tan\epsilon\,[1 + \cos 2(\epsilon - \theta)] - \frac{2}{n}[\sin\epsilon - \sin(\epsilon - \theta)]\right\}, \tag{6.6}$$

$$\Psi = \frac{1}{n\cos^2\epsilon}\left\{2(1 - \cos\theta)\cos(\epsilon - \theta) + \frac{1}{n}[\sin\epsilon - \sin(\epsilon - \theta)]^2\right\}. \tag{6.7}$$

Equations (6.5)-(6.7) yield the curve family ϵ = const. in Fig. 2. To obtain the curve corresponding to $\epsilon = 0$, we set $\epsilon = 0$ in (6.6) and (6.7). We then compute the values of Φ and Ψ corresponding to $\theta = 0°$, $5°$, $10°$, $\cdots$, $90°$. Equation (6.5) then yields the values of ρ corresponding to these values of θ. The curve $\epsilon = 0$ can then be constructed by point plotting. A similar procedure yields the curves corresponding to $\epsilon = 5°$,

10°, 15°, ••• , 45°. However, in each of these cases θ = 0°, 5°, 10°, ••• , 90° + ϵ.

The numerical computations involved here are rather extensive. Subsequent portions of this study, (Section 8) require the constructions of members of the curve family ϵ = cost. for a denser set of values of ϵ. In particular, only portions of these curves in the vicinity of the place where ρ has a maximum value are required. The computations for these additional curves were not carried out as previously but were made by use of the results of the previous computations and use of the forward and backward finite-difference formulas of Newton. For example, previous calculations yielded the values of ρ corresponding to θ = 40°, ϵ = 0°, 5°, 10°, ••• , 45°. The two difference formulas mentioned above then readily yield the values of ρ corresponding to θ = 40°, ϵ = 2.5°, 7.5°, 12.5°, ••• , 42.5°.

SECTION 7: FIGURE 2

THEORY FOR THE CURVE $\rho = \rho_{max}$

Equations (6.5)-(6.7) express the modified range ρ in terms of the pull-up angle θ and the angle of approach ϵ when the bomb bursts on the target. For convenience, we write (6.5) in the form

$$\rho = \rho(\theta, \epsilon). \tag{7.1}$$

Corresponding to each value of ϵ there is a value of ρ which is as large as possible; it is denoted by ρ_{max}; to obtain ρ_{max} we could solve simultaneously Equation (7.1) and the equation

$$\frac{\partial \rho}{\partial \theta} = 0 \tag{7.2}$$

for ρ and θ in terms of ϵ. The values of ρ thus obtained are the desired values of ρ_{max}.

A casual glance at (6.5)-(6.7) indicates that the solving of these two simultaneous equations (7.1) and (7.2) would present severe algebraic difficulties, and if a numerical method of solution were employed, the numerical work would be prohibitive. Accordingly, the following numerical approach, which is only approximate, is employed. In the determination of the curves ϵ = const. in Fig. 2 (Section 6), the coordinates of points on the curves

ϵ = const. are computed and the curves ϵ = const. are thus constructed by point plotting. On the curve $\epsilon = 0$, we select the three points nearest the point where $\rho = \rho_{max}$. Let us denote these three by $P_1(\rho_1, \theta_1)$, $P_2(\rho_2, \theta_2)$, and $P_3(\rho_3, \theta_3)$ in order of increasing θ. Through these three points we pass a parabola with a horizontal axis. In the language of finite differences, the equation of this parabola is

$$\rho(\theta) = \rho_1 + p\,\Delta\rho_1 + \frac{p(p-1)}{2}\,\Delta^2\rho_1, \tag{7.3}$$

where

$$\Delta\rho_1 = \rho_2 - \rho_1,\ \Delta\rho_2 = \rho_3 - \rho_2,\ \Delta^2\rho_1 = \Delta\rho_2 - \Delta\rho_1,$$

$$p = \frac{\theta - \theta_1}{w},\ w = \theta_2 - \theta_1 = \theta_3 - \theta_2.$$

Let $\bar{P}(\bar{\rho}, \bar{\theta})$ be that point on this parabola where ρ is as large as possible. From (7.3) it readily follows that

$$\bar{\rho} = \rho_1 + \bar{p}\,\Delta\rho_1 + \frac{\bar{p}(\bar{p}-1)}{2}\,\Delta^2\rho_1,\ \bar{\theta} = \theta_1 + w\bar{p}, \tag{7.4}$$

where

$$\bar{p} = \frac{1}{2} - \frac{\Delta\rho_1}{\Delta^2\rho_1}. \tag{7.5}$$

We then compute the coordinates of that point $\tilde{P}$, on the curve $\epsilon = 0$ where $\theta = \bar{\theta}$ and denote the ρ coordinate of this point by $\tilde{\rho}$. Then $\tilde{P}$ has coordinates $(\tilde{\rho}, \bar{\theta})$. Of the four points P_1, P_2, P_3, and $\tilde{P}$, we then select the three which are closest to the point where $\rho = \rho_{max}$ and repeat the process until stability in the values of $\tilde{\rho}$ is reached. The final value of $\tilde{\rho}$ thus obtained is ρ_{max} corresponding to $\epsilon = 0$. A similar procedure yields ρ_{max} for $\epsilon = 5°, 10°, \cdots, 45°$.

In practice it is found that the difference of $\bar{\rho}$ and $\tilde{\rho}$ for the first cycle is negligible, due to the fact that P_1, P_2 and P_3 are close together. Hence, it follows that ρ_{max} is given with satisfactory accuracy by the value of $\bar{\rho}$ given by (7.4) and the value of θ corresponding to ρ_{max} is given also with satisfactory accuracy by (7.4).

In the above computations the pull-up constant n had the value 3. When $\epsilon = 0$, it appears from the numerical computations that $\rho_{max} = 4/3$.

Computations made for an earlier study indicate that $\rho_{max} = 3/2$ when $n = 2$. Accordingly, a theoretical determination was attempted for ρ_{max} when $\epsilon = 0$. After some very extensive and involved algebra, it was found that

$$\rho_{max} = \frac{n+1}{n} \tag{7.6}$$

when $\epsilon = 0$. A similar determination of ρ_{max} for general values of ϵ was abandoned early because of the algebraic complexity.

SECTION 8: FIGURE 2

THEORY FOR THE CURVE FAMILY T = CONST.

To find the equation from which this curve family can be deduced by computation, we must eliminate ϵ between the fundamental equations (3.6) and (3.7). Just as in Section 6, we shall defer setting ξ_B and ζ_B equal to zero for the present, even though we are concerned only with the case when the bomb burst on the target. To carry out the elimination of ϵ between (3.6) and (3.7), we write these equations in the form

$$\left.\begin{aligned} \alpha_1 \sin\epsilon + \beta_1 \cos\epsilon &= \gamma_1, \\ \alpha_2 \sin\epsilon + \beta_2 \cos\epsilon &= \gamma_2, \end{aligned}\right\} \tag{8.1}$$

where

$$\left.\begin{aligned} \alpha_1 = -\beta_2 &= \frac{1}{n} - \frac{1}{n}\cos\theta + T\sin\theta, \\ \beta_1 = \alpha_2 &= -\rho + \frac{1}{n}\sin\theta + T\cos\theta, \\ \gamma_1 = -\rho\,\xi_B,\ \gamma_2 &= -\rho\,\zeta_B - \frac{1}{2}T^2. \end{aligned}\right\} \tag{8.2}$$

Next, we solve (8.1) for $\sin\epsilon$ and for $\cos\epsilon$, then square and add the results to obtain the equation

$$\alpha_1^2 + \beta_1^2 = \gamma_1^2 + \gamma_2^2. \tag{8.3}$$

Substitution in (8.3) from (8.2) then yields

$$\rho^2 - 2\phi\rho + \psi = 0, \tag{8.4}$$

where

$$\phi = \frac{1}{1 - \xi_B^2 - \zeta_B^2}\left(\frac{1}{n}\sin\theta + T\cos\theta + \frac{1}{2}\zeta_B T^2\right), \tag{8.5}$$

$$\psi = \frac{1}{1 - \xi_B^2 - \zeta_B^2}\left[\frac{2}{n^2}(1 - \cos\theta) + \frac{2T}{n}\sin\theta + T^2 - \frac{1}{4}T^4\right]. \tag{8.6}$$

Solving (7.4) for ρ, we obtain

$$\rho = \phi \pm \sqrt{\phi^2 - \psi}\,. \tag{8.7}$$

One value of ρ given by this equation is extraneous. To resolve this, we note that (8.7) yields values of ρ corresponding to given θ and T. Intuitively it follows that there will be two values, one corresponding to a positive ϵ and one to a negative ϵ. The positive ϵ will yield a value of ρ larger than will the negative ϵ. Hence, in (8.3) we choose the positive sign to obtain

$$\rho = \phi + \sqrt{\phi^2 - \psi}\,. \tag{8.8}$$

When the bomb bursts on the target, we have $\xi_B = \zeta_B = 0$ so that (8.5) and (8.6) yield

$$\phi = \frac{1}{n}\sin\theta + T\cos\theta, \tag{8.9}$$

$$\psi = \frac{2}{n^2}(1 - \cos\theta) + \frac{2T}{n}\sin\theta + T^2 - \frac{1}{4}T^4. \tag{8.10}$$

Equations (8.8) - (8.10) yield the curve family T = const. in Fig. 2. To obtain the curve corresponding to T = 0.5 in Fig. 2, we set T = 0.5 in (7.9) and (7.10). We then compute the values of ϕ and ψ corresponding to θ = 0°, 5°, 10°, ••• . Equation (8.8) then yields the values of ρ corresponding to these values of θ. The curve T = 0.50 can then be constructed

by point plotting. A similar procedure yields the curves corresponding to $T = 1.00, 1.25, 1.50, \cdots, 3.00$.

SECTION 9: FIGURE 2

THEORY FOR THE CURVE FAMILY Q = CONST.

Let us refer to Fig. 3 which, like Fig. 1, represents a typical bombing run. The airplane is closest to the ground when it is at the point M. The minimum ground clearance is thus the y-coordinate q of M. From Fig. 3 we see that

$$q = R_o \sin \epsilon - r (1 - \cos \epsilon).$$

Substitution for r from (2.1) then yields

$$q = R_o \sin \epsilon - \frac{V^2}{ng} (1 - \cos \epsilon). \tag{9.1}$$

We now introduce the dimensionless ground clearance Q defined by the relation

$$Q = q/L', \tag{9.2}$$

where L' is the standard length defined in Section 3. Substitution in (9.1) for q from (9.2) and for R_o from (3.2) then yields, since $V^2/g = L$,

$$Q = \rho \sin \epsilon - \frac{1}{n} (1 - \cos \epsilon).$$

Solving for ρ, we obtain

$$\rho = \frac{Q + \frac{1}{n} (1 - \cos \epsilon)}{\sin \epsilon}. \tag{9.3}$$

Equation (9.3) yields the curve family Q = const. in Fig. 2. Of course, n has the value three throughout this study. To obtain the curve corresponding to Q = 0.1, we set Q = 0.1 in (9.3), then compute the values of

ρ corresponding to $\epsilon = 0°, 5°, 10°, \cdots, 45°$. On the curves $\epsilon = 0°, 5°, 10°, \cdots, 45°$ in Fig. 2, we then locate the points corresponding to these values of ρ, and through these points we draw a smooth curve; it is the curve $Q = 0.1$. We proceed similarly for $Q = 0.3, 0.5, \cdots, 2.7$.

In carrying out the procedure described in the previous paragraph, we find that, in the vicinity of the curve $\rho = \rho_{max}$, points were not obtained with a density sufficient to permit an accurate drawing of the curves $Q =$ const. In order to remove this obstruction, use was made of the curves of the family $\epsilon =$ const. computed for a denser set of values of ϵ by the use of finite differences, as described in the last paragraph of Section 6. These curves have not been reproduced in Fig. 2 since they would complicate this figure still further.

SECTION 10: FIGURE 4

EXPLANATIONS

Figures 4a and 4b present in convenient form information concerning the various bombing runs specified by assigned values of the modified coordinates (λ, μ) of the airplane at the point O (Fig. 1) where the pull-up begins. Figures 4a and 4b deal with a situation in which the bomb bursts on the target and the airplane makes a 3g turn in travelling on the circular arc OR (Fig. 1).

In Figs. 4a and 4b, λ is plotted horizontally and μ is plotted vertically. It thus appears that to each point in some region in the (λ, μ) plane of Figs. 4a and 4b there corresponds either one or two bombing runs, depending on circumstances. When two bombing runs correspond to a single point in the (λ, μ) plane, we distinguish them by referring to one as being of S-type and the other as being of L-type; S-type is characterized by having smaller values of the pull-up angle Θ and of the time of flight T than does L-type. Figure 4a presents information concerning bombing runs of S-type, while Fig. 4b refers to bombing runs of L-type.

In Figs 4a and 4b there are four families of curves and a single curve besides. These will now be explained in turn.

The Family $\epsilon =$ Const.—As mentioned above, to each bombing run there corresponds a point in the (λ, μ) plane of Figs. 4a and 4b. The curves $\epsilon =$ const. in Figs. 4a and 4b indicate the values of the angle of approach ϵ associated with the various bombing runs. The theory leading to the determination of the curves of this family is developed in Section 12.

The Curve $\rho = \rho_{max}$.—To each bombing run there corresponds a point on the (λ, μ) plane of Figs. 4a and 4b. The points on the curves $\rho = \rho_{max}$ of these figures correspond to bombing runs for which the angle of approach ϵ is assigned and the modified range ρ is as large as possible. The theory leading to the determination of these curves is developed in Section 13. It will be noted that these curves form right-hand boundaries of the regions in the (λ, μ) plane of Figs. 4a and 4b made up of points corresponding to which bombing runs exist.

The Family T = Const.—It will be recalled that T is the modified time of free flight of the bomb. To each bombing run there corresponds a point in the (λ, μ) plane of Figs. 4a and 4b. The curves T = const. in these figures indicate the values of T associated with the various bombing runs. It will be noted that, provided T is large enough, a curve T = const. has branches in both Figs. 4a and 4b. Both branches terminate at the same point on the curve $\rho = \rho_{max}$ and are tangent to this curve. The theory leading to the determination of the curves of the family T = const. is developed in Section 14.

The Family Q = Const.—It will be recalled that Q is the modified minimum ground clearance of the airplane and is defined in Equation (8.2). To each bombing run there corresponds a point in the (λ, μ) plane of Figs. 4a and 4b. The curves Q = const. in these figures indicate the values of Q associated with the various bombing runs. The theory leading to the determination of the curves of this family is developed in Section 15.

The Family θ = Const.—It will be recalled that θ is the pull-up angle of the airplane. To each bombing run there corresponds a point in the (λ, μ) plane of Figs. 4a and 4b. The curves θ = const. in these figures indicate the values of θ associated with the various bombing runs. It will be noted that, provided θ is large enough, a curve θ = const. has branches in both Figs. 4a and 4b. Both branches terminate at the same point on the curve $\rho = \rho_{max}$ and are tangent to this curve. The theory leading to the determination of the curves of this family is developed in Section 16.

SECTION 11: FIGURE 4

AN EXAMPLE OF ITS USE

Let us suppose an airplane approaches the target at 1000 ft/sec^{-1} and begins the pull-up when the horizontal range is 60,000 ft and the altitude is 30,000 ft. It will be recalled that in all bombing runs considered in this study the airplane is aimed directly at the target at the instant when the

pull-up begins, so the information given above is enough to specify two bombing runs, one of S-type and one of L-type, as defined in Section 10, par. 2.

For convenience we take $g = 32$ ft/sec^{-2}, whence the standard length L' and the standard time T' have the values $L' = V^2/g = 31{,}250$ ft and $T' = V/g = 31.250$ sec. The modified coordinates of the airplane at pull-up beginning are thus

$$\lambda = \frac{x}{L'} = \frac{60{,}000}{31{,}250} = 1.920, \quad \mu = \frac{y}{L'} = \frac{30{,}000}{31{,}250} = .960.$$

The point corresponding to these values of λ and μ is marked A in Fig. 4a and B in Fig. 4b.

The point A refers to a bombing run of S-type. By means of linear interpolation, we obtain from Fig. 4a for the point A the values $\epsilon = 26.6°$, $\theta = 47.7°$, $T = 1.77$, and $Q = .928$. Hence, the angle of approach is 26.6°, the pull-up angle is 47.7°, the time of flight of the bomb is $TT' = 1.77 \times 31.25 = 55.3$ sec, and the minimum ground clearance is $QL' = .928 \times 31{,}250 = 290 \times 100$ ft.

The point B refers to a bombing run of L-type. By means of linear interpolation, we obtain from Fig. 4b for the point B the values $\epsilon = 26.6°$, $\theta = 78.3°$, $T = 2.42$, and $Q = .928$. Hence, the angle of approach is 24.4°, the pull-up angle is 78.3°, the time of flight of the bomb is $TT' = 2.42 \times 31.25 = 75.6$ sec, and the minimum ground clearance is $QL' = .928 \times 31{,}250 = 290 \times 100$ ft.

SECTION 12: FIGURE 4

THEORY FOR THE CURVE FAMILY ϵ = CONST.

Let us refer to the typical bombing run illustrated in Fig. 1, Section 1. If (x, y) denote the coordinates of the point O where the pull-up begins, then

$$y = x \tan \epsilon. \qquad (12.1)$$

But, by (3.3) we have $x = \lambda L'$ and $y = \mu L'$, where L' is the standard length defined in Section 3. Substitution for x and y from these equations in (12.1) then yields

$$\mu = \lambda \tan \epsilon. \qquad (12.2)$$

This equation gives the family of curves ϵ = const. in Figs. 4a and 4b. The family obviously consists of straight lines passing through the origin.

SECTION 13: FIGURE 4

THEORY FOR THE CURVE $\rho = \rho_{max}$

Corresponding to each value of the angle of approach ϵ, there is a value of the modified slant range ρ which is as large as possible. This value is denoted by ρ_{max}, and its determination was discussed in detail in Section 7. To obtain the curves $\rho = \rho_{max}$ in Figs 4a and 4b, we measure off, along the lines ϵ = const. in these figures, distances equal to the corresponding values of ρ_{max}; a smooth curve is then drawn through the points thus obtained; it is the desired curve.

SECTION 14: FIGURE 4

THEORY FOR THE CURVE FAMILY T = CONST.

To find the equation from which this curve family can be deduced by computation, we must eliminate θ between the fundamental equations (3.6) and (3.7). Since we are concerned only with the case in which the bomb bursts on the target, we set $\xi_B = \zeta_B = 0$, and then write (3.6) and (3.7) in the form

$$\left.\begin{aligned} -\frac{1}{n}\sin(\epsilon-\theta) + T\cos(\epsilon-\theta) &= \rho\cos\epsilon - \frac{1}{n}\sin\epsilon, \\ T\sin(\epsilon-\theta) + \frac{1}{n}\cos(\epsilon-\theta) &= \rho\sin\epsilon + \frac{1}{n}\cos\epsilon - \frac{1}{2}T^2. \end{aligned}\right\} \qquad (14.1)$$

We now square and add the two equations in (14.1) to obtain

$$T^2 = \rho^2 + \frac{1}{4}T^4 - T^2\left(\rho\sin\epsilon + \frac{1}{n}\cos\epsilon\right)$$

or

$$\rho^2 - 2\bar{\phi}\rho + \bar{\psi} = 0, \tag{14.2}$$

where

$$\bar{\phi} = \frac{1}{2} T^2 \sin \epsilon, \quad \bar{\psi} = \frac{1}{4} T^4 - T^2 \left(1 + \frac{1}{n} \cos \epsilon\right). \tag{14.3}$$

Solving (13.2) for ρ, we obtain

$$\rho = \bar{\phi} \pm \sqrt{\bar{\phi}^2 - \bar{\psi}}. \tag{14.4}$$

To obtain the curve T = .5 in Fig. 4, we compute from (14.4) the values of ρ corresponding to T = .5 and ϵ = 0°, 5°, 10°, ••• , 45°. We find that the negative sign in (14.4) yields negative values for ρ which are extraneous. We measure off, along the lines ϵ = 0°, 5°, 10°, ••• , 45° in Fig. 4, distances equal to the values of ρ computed above. A smooth curve is then drawn through the points so obtained; it is the curve T = .50. A similar procedure yields the curves T = .75, 1.00, 1.25, ••• , 3.00, but for the higher values of T it is found that (14.4) yields two positive values of ρ.

For the higher values of T, the curves T = const. are tangent to the curve $\rho = \rho_{max}$. The points of tangency divide these curves into two parts; one part appears in Fig. 4a and the other in Fig. 4b. The parts in Figs. 4a and 4b relate to bombing runs of S-type and L-type, respectively. It will be recalled that for a given point of pull-up beginning there are, in general, two bombing runs possible, the one with the smaller pull-up angle θ being of S-type and the one with larger pull-up angle being of L-type.

SECTION 15: FIGURE 4

THEORY FOR THE CURVE FAMILY Q = CONST.

The modified ground clearance Q is defined in Section 9 by the relation $Q = q/L'$, where q is the actual minimum ground clearance of the airplane and L' is the standard length defined in Section 3. In Section 9 we found that

$$\rho = \frac{Q + \frac{1}{3}(1 - \cos \epsilon)}{\sin \epsilon}. \tag{15.1}$$

To obtain the curve corresponding to $Q = 0.1$, we set $Q = 0.10$ in (15.1) and then compute the values of ρ corresponding to $\epsilon = 0°, 5°, 10°, \cdots, 45°$. (These values have already been computed in Section 9.) On the straight lines $\epsilon = 0°, 5°, \cdots, 45°$ in Figs. 4a and 4b, we measure off from the origin distances equal to the values of ρ so computed. Through the points so obtained, we draw a smooth curve; it is the curve $Q = 0.1$. In similar fashion we get the curves $Q = 0.3, 0.5, \cdots, 2.7$.

SECTION 16: FIGURE 4

THEORY FOR THE CURVE FAMILY Θ = CONST.

In Section 6 we developed (6.5) which reads

$$\rho = \Phi + \sqrt{\Phi^2 - \Psi}, \qquad (16.1)$$

where Φ and Ψ are certain known functions of Θ and ϵ given in (6.5) and (6.6). To obtain the curve corresponding to $\Theta = 10°$, we set $\Theta = 10°$ in (16.1) and then compute the values of ρ corresponding to $\epsilon = 0°, 5°, 10°, \cdots, 45°$. (These values have already been computed in Section 6.) On the straight lines $\epsilon = 0°, 5°, 10°, \cdots, 45°$ in Fig. 4, we measure off from the origin distances equal to the values of ρ so computed. Through the points so obtained, we draw a smooth curve; it is the curve $\Theta = 10°$. In similar fashion we get the curves $\Theta = 20°, 30°, \cdots, 120°$.

For the higher values of Θ, the curves Θ = const. are tangent to the curve $\rho = \rho_{max}$. The points of tangency divide these curves into two parts; one part appears in Fig. 4a and the other in Fig. 4b. The parts in Figs. 4a and 4b relate to bombing runs of S-type and L-type, respectively. It will be recalled that for a given point of pull-up beginning there are, in general, two bombing runs possible, the one with the smaller pull-up angle Θ being of S-type and the one with the larger pull-up angle being of L-type.

SECTION 17: FIGURE 5

EXPLANATIONS

Figures 5a and 5b present in convenient form information concerning the various bombing runs specified by assigned values of the modified coordin-

ates (λ, μ) of the airplane at the point R (Fig. 1) where the bomb is released. Figures 5a and 5b deal with a situation in which, as usual, the bomb bursts on the target and the airplane makes a 3g turn in travelling on the circular arc OR (Fig. 1).

In Figs. 5a and 5b, λ is plotted horizontally and μ is plotted vertically. It thus appears that to each point in some region in the (λ, μ) plane of Figs. 5a and 5b there corresponds either one or two bombing runs, depending on circumstances. When two bombing runs correspond to a single point in the (λ, μ) plane, we distinguish them, just as in Section 10, by referring to one as being of S-type and the other as being of L-type; by definition, S-type has a smaller value for the pull-up angle θ than does L-type. Figure 5a presents information concerning bombing runs of S-type, while Fig. 5b refers to bombing runs of L-type.

In Figs. 5a and 5b there are four families of curves and two single curves besides. These will now be explained in turn.

The Family ϵ = Const.—As mentioned above, to each bombing run there corresponds a point in the (λ, μ) plane of Figs. 5a and 5b. The curves ϵ = const. in these figures indicate the values of the angle of approach ϵ associated with the various bombing runs. The theory leading to the determination of the curves of this family is developed in Section 19. It is found that the family of curves ϵ = const. has an envelope E and that each point to the left of E corresponds to two different bombing runs, one of S-type and one of L-type. The S-type bombing runs are described in Fig. 5a and the L-type are described in Fig. 5b. As usual, the S-type bombing run has a smaller pull-up angle than has the L-type bombing run.

The Curve $\rho = \rho_{max}$.—To each bombing run there corresponds a point in the (λ, μ) plane of Figs. 5a and 5b. The points on the curve $\rho = \rho_{max}$ of Fig. 5b correspond to bombing runs for which the angle of approach ϵ is assigned and the modified range ρ is as large as possible. The theory leading to the determination of this curve is developed in Section 20. It will be noted that, unlike Figs. 4a and 4b the curve $\rho = \rho_{max}$ lies entirely in Fig. 5b and does not form a right-hand boundary of the region in the (λ, μ) plane of Figs. 5a and 5b made up of points corresponding to which bombing runs exist.

The Family ρ = Const.—As mentioned above, to each bombing run there corresponds a point in the (λ, μ) plane of Figs. 5a and 5b. The curves ρ = const. in these figures indicate the values of the modifed slant range ρ associated with the various bombing runs. The theory leading to the determination of the curves of this family is developed in Section 21. The family of curves ρ = const. has the curve E as an envelope, and E divides the curves of the family into two parts, one in Fig. 5a and one in Fig. 5b.

The Family $\epsilon - \theta = \text{Const.}$—To each bombing run there corresponds a point in the (λ, μ) plane of Figs. 5a and 5b. The curves $\epsilon - \theta = \text{const.}$ in these figures indicate the values of $\epsilon - \theta$ associated with the various bombing runs. Now ϵ is the angle of approach of the airplane and θ is the pull-up angle of the airplane, so $\epsilon - \theta$ is the angle which the axis of the airplane makes with the horizontal at the instant when the bomb is released. We note that this angle is positive when the airplane is diving and is negative when the airplane is climbing. We shall refer to this angle as the attitude of the airplane. The theory leading to the determination of the curves of the family $\epsilon - \theta = \text{const.}$ is developed in Section 22. The family of curves $\epsilon - \theta = \text{const.}$ has the curve E as an envelope, and E divides the curves of the family into two parts; one part appears in Fig. 5a and the other in Fig. 5b.

The Family $Q = \text{Const.}$—As mentioned before, to each bombing run there corresponds a point in the (λ, μ) plane of Figs. 5a and 5b. Now Q is the modified minimum ground clearance of the airplane, and the curves $Q = \text{const.}$ in Figs. 5a and 5b indicate the values of Q associated with the various bombing runs. The theory leading to the determination of the curves of the family $Q = \text{const.}$ is developed in Section 23. The family of curves $\epsilon - \theta = \text{const.}$ has the curve E as an envelope, and E divides the curves of the family into two parts; one part appears in Fig. 5a and the other in Fig. 5b.

SECTION 18: FIGURE 5

AN EXAMPLE OF ITS USE

Let us suppose an airplane approaches the target at 1000 ft/sec^{-1} and releases the bomb when the horizontal range is 45,000 ft and the altitude is 30,000 ft. This information is enough to specify two bombing runs, one of S-type and one of L-type, as defined in Section 17, par. 2.

For convenience we take $g = 32\ \text{ft/sec}^{-2}$, whence the standard length L' and the standard time T' have the values $L' = V^2/g = 31{,}250$ ft and $T' = V/g = 31.250$ sec. The modified coordinates of the airplane at the instant of bomb release are thus

$$\lambda = \frac{x}{L'} = \frac{45{,}000}{31{,}250} = 1.440, \quad \mu = \frac{y}{L'} = \frac{30{,}000}{31{,}250} = .960.$$

The point corresponding to these values of λ and μ is marked A in Fig. 5a and B in Fig. 5b.

The point A refers to a bombing run of S-type. By means of linear interpolation, we obtain from Fig. 5a for the point A the values $\epsilon = 31.7°$,

$\epsilon - \theta = -3.4°$, $Q = .96$, and $\rho = 1.92$. Hence, the angle of approach ϵ has the value 31.7°, the pull-up angle θ has the value 35.1°, the minimum ground clearance is $QL' = .96 \times 31{,}250 = 30 \times 1000$ ft, and the range at pull-up beginning is $\rho L' = 1.92 \times 31{,}250 = 600 \times 100$ ft.

The point B refers to a bombing run of L-type. By means of linear interpolation, we obtain from Figs. 5b for the point B the values $\epsilon = 24.8°$, $\epsilon - \theta = -52.7$, $Q = .83$, and $\rho = 2.04$. Hence, the angle of approach ϵ is 24.8°, the pull-up angle θ is 77.5°, the minimum ground clearance is $QL' = .83 \times 31{,}250 = 26 \times 1000$ ft, and the range at pull-up beginning is $\rho L' = 2.04 \times 31{,}250 = 638 \times 100$ ft.

SECTION 19: FIGURE 5

THEORY FOR THE CURVE FAMILY ϵ = CONST.

Let us return to the typical bombing run illustrated in Fig. 1, Section 1. Let (x, y) denote the coordinates of the point R where the bomb is released. Expressions for the coordinates of R were deduced in Section 2 and are expressed in (2.2). Hence, we have

$$\left.\begin{aligned} x &= R_o \cos\epsilon - r \sin\epsilon + r \sin(\epsilon - \theta), \\ y &= R_o \sin\epsilon + r \cos\epsilon - r \cos(\epsilon - \theta). \end{aligned}\right\} \qquad (19.1)$$

Let (λ, μ) denote the modified coordinates of R. Then,

$$\lambda = x/L', \quad \mu = y/L', \qquad (19.2)$$

where L' is the usual standard length, defined by the relation $L' = V^2/g$, V being the velocity of the airplane, and g being the usual acceleration due to gravity. The modified slant range ρ is also defined in terms of the actual slant range R_o (Fig. 1) by the relation

$$\rho = R_o/L', \qquad (19.3)$$

and the radius r of the circular portion of the path of the airplane is given

by (2.1) which reads

$$r = V^2/ng, \tag{19.4}$$

since the airplane travels this path with a radial acceleration of ng. Because $V^2/g = L'$, then (19.4) becomes

$$r = L'/n. \tag{19.5}$$

Substitution in (19.1) for x, y, R_o, and r from (19.2), (19.3) and (19.5) then yields

$$\left.\begin{aligned} \lambda &= \rho \cos \epsilon - \frac{1}{n}[\sin \epsilon - \sin (\epsilon - \theta)], \\ \mu &= \rho \sin \epsilon + \frac{1}{n}[\cos \epsilon - \cos (\epsilon - \theta)]. \end{aligned}\right\} \tag{19.6}$$

To obtain the curves in Figs. 5a and 5b corresponding to $\epsilon = 0$, we set $\epsilon = 0$ and also set $\theta = 0°, 5°, 10°, \cdots, 90°$. In Section 6 the values of ρ corresponding to these values of ϵ and θ were computed. If these values of ϵ, θ, and ρ are substituted into the right sides of (19.6), we obtain 19 pairs of values of (λ, μ) corresponding to $\epsilon = 0$ and $\theta = 0°, 5°, 10°, \cdots, 90°$. By point plotting we then get 19 points in the (λ, μ) plane of Fig. 5. A smooth curve is now drawn through these points; it is the curve $\epsilon = 0$. A similar procedure yields the curves corresponding to $\epsilon = 5°, 10°, \cdots, 45°$. However, in each of these cases, $\theta = 0°, 5°, 10°, \cdots, 90° + \epsilon$.

The family of curves ϵ = const. has an envelope which we denote by E. The curves ϵ = const. are, of course, tangent to this envelope, and the points of tangency divide these curves into two parts; one part appears in Fig. 5a and the other in Fig. 5b. Just as in the case of Fig. 4, the bombing runs described in Fig. 5a are said to be of S-type and those in Fig. 5b are said to be of L-type. In order to appreciate fully the distinction between these two types, we must realize that corresponding to each point of missile release there is a point in Fig. 5a and a point similarly situated in Fig. 5b; however, the bombing runs corresponding to these two points are quite different; the bombing run corresponding to the point in Fig. 5a is of S-type and has a pull-up angle smaller than has the bombing run of L-type corresponding to the point in Fig. 5b.

SECTION 20: FIGURE 5

THEORY FOR THE CURVE $\rho = \rho_{max}$

To obtain the curve $\rho = \rho_{max}$ in Fig. 5, we set $\epsilon = 0°, 5°, 10°, \cdots, 45°$. Corresponding to each of these values there is a maximum value of ρ and a corresponding value of θ, which values were computed in Section 7. If, in the right side of (19.6), we insert these values of ϵ, ρ, and θ, a set of 10 pairs of values of (λ, μ) is obtained. By point plotting we then get 10 points in Fig. 5b. A smooth curve is then drawn through these 10 points; it is the curve $\rho = \rho_{max}$.

SECTION 21: FIGURE 5

THEORY FOR THE CURVE FAMILY ρ = CONST.

In Section 6 the modified slant range ρ was determined in terms of the angle of approach ϵ and the pull-up angle θ. This result is expressed in (6.5) which reads,

$$\rho = \Phi + \sqrt{\Phi^2 - \Psi}, \qquad (21.1)$$

where Φ and Ψ are certain complicated functions of ϵ and θ given in (6.6) and (6.7). To obtain the curves in Figs. 5a and 5b corresponding to $\rho = .5$, we must set $\rho = .5$ and $\epsilon = 0°, 5°, \cdots, 45°$ in (21.1). We then compute the corresponding values of θ. If these values of ρ, ϵ, and θ are substituted into the right sides of (19.6), we obtain 10 pairs of values of the modified coordinates (λ, μ) of the airplane at the instant of missile release. By point plotting we then get 10 points in the (λ, μ) plane of Fig. 5. A smooth curve is now drawn through these points; it is the curve $\rho = .5$. It will be noted that this curve is tangent to the envelope E; the point of tangency divides this curve into two parts, one of which appears in Fig. 5a and the other in Fig. 5b. A similar procedure yields the curves $\rho = .75, 1.00, 1.25, \cdots, 4.00$.

As mentioned in the previous paragraph, (21.1) expresses ρ as a complicated function of ϵ and θ. Also, the procedure outlined in the previous paragraph involves the assigning of values to ρ and ϵ and the computation of the corresponding values of θ. Because of the complexity of the right side of

(21.1), a direct computation of this is impractical, and, instead, the method of finite differences is applied to the values obtained in Section 6 for ρ corresponding to assigned values of θ and ϵ. In order to describe the actual finite-difference procedure used, we denote the assigned values of ϵ and ρ by $\bar{\epsilon}$ and $\bar{\rho}$ and the corresponding computed value of θ by $\bar{\theta}$. Further, let us denote (21.1) by writing

$$\rho = \rho(\theta, \epsilon). \tag{21.2}$$

To obtain $\bar{\theta}$, we would normally approximate the relation $\rho = \rho(\theta, \bar{\epsilon})$ by an expression of the form

$$\theta = \text{polynomial in } \rho. \tag{21.3}$$

Now the curves $\rho = \rho(\theta, \bar{\epsilon})$ appear in Fig. 2 and cannot be approximated well by (21.3) in regions where their slope is large. Further, the coefficients on the right side of (21.3) can be computed only by use of divided differences, which makes extra labor. Hence, the relation $\rho = \rho(\theta, \bar{\epsilon})$ was approximated by an expression of the form

$$\rho = \text{quadratic in } \theta. \tag{21.4}$$

This amounts to replacing the curve $\rho = \rho(\theta, \bar{\epsilon})$ by a parabola with a horizontal axis.

Let $(\rho_1, \theta_1, \bar{\epsilon})$, $(\rho_2, \theta_2, \bar{\epsilon})$, and $(\rho_3, \theta_3, \bar{\epsilon})$ be three adjacent sets of values computed in Section 6 and such that $\bar{\rho}$ is bracketed by ρ_1, ρ_2, and ρ_3. In the usual notation we have

$$\Delta_1 \rho_1 = \rho_2 - \rho_1, \quad \Delta_1 \rho_2 = \rho_3 - \rho_2,$$

$$\Delta_2 \rho_1 = \Delta_1 \rho_2 - \Delta_1 \rho_1, \quad \Delta \theta = \theta_2 - \theta_1 = \theta_3 - \theta_2.$$

Equation (21.4) is now explicitly

$$\rho = \rho_1 + p \Delta_1 \rho_1 + \frac{1}{2} p(p - 1) \Delta_2 \rho_1, \quad p = \frac{\theta - \theta_1}{\Delta\theta}. \tag{21.5}$$

If in (21.5) we set $\rho = \bar{\rho}$ and $\theta = \bar{\theta}$ and solve the resulting equation for $\bar{\theta}$, we obtain

$$\bar{\theta} = \theta_1 + p \cdot \Delta\theta, \tag{21.6}$$

where

$$p = b \pm \sqrt{b^2 - c}, \tag{21.7}$$

$$b = \frac{1}{2} - \frac{\Delta_1 \rho_1}{\Delta_2 \rho_1}, \quad c = -2\frac{\bar{\rho} - \rho_1}{\Delta_2 \rho_1}. \tag{21.8}$$

In (21.7) we choose the sign which puts p in the range $0 < p < 2$. Sometimes both signs must be used. Equation (21.6) thus gives the value $\bar{\theta}$ of θ corresponding to an assigned value $\bar{\rho}$ of ρ.

SECTION 22: FIGURE 5

THEORY FOR THE CURVE FAMILY $\epsilon - \theta$ = CONST.

In Section 19 the values of (λ, μ) were computed for $\epsilon = 0°, 5°, 10°, \cdots, 45°$ and for $\theta = 0°, 5°, 10°, \cdots, 90° + \epsilon$. From these computations we can read the values of (λ, μ) corresponding to $\epsilon - \theta = 40°$. By point plotting we then get a set of points in the (λ, μ) plane of Fig. 5. A smooth curve is now drawn through these points; it is the curve $\epsilon - \theta = 40°$. A similar procedure yields the curves $\epsilon - \theta = 35°, 30°, 25°, \cdots, -90°$. As mentioned in Section 17, the angle $\epsilon - \theta$ is the angle which the axis of the airplane makes with the horizontal at the instant of missile release. It then follows that the curve $\epsilon - \theta = -90°$ corresponds to the case where the bomb is released vertically upward from points directly over the target. The curve $\epsilon - \theta = -90°$ is thus the curve $\lambda = 0$, as can be seen from Fig. 5.

It will be noted that some of the curves $\epsilon - \theta$ = const. are tangent to the envelope E; the point of tangency divides such curves into two parts, one of which appears in Fig. 5a and the other in Fig. 5b.

SECTION 23: FIGURE 5

THEORY FOR THE CURVE FAMILY Q = CONST.

The modified ground clearance Q is defined in Section 9 by the relation $Q = q/L'$, where q is the actual minimum ground clearance and L' is the standard length defined in Section 3. In Section 9 we found that

$$\rho = \frac{Q + \frac{1}{n}(1 - \cos \epsilon)}{\sin \epsilon} \tag{23.1}$$

and in Section 6 we found that

$$\rho = \Phi + \sqrt{\Phi^2 - \Psi} = \rho(\theta, \epsilon), \tag{23.2}$$

where Φ and Ψ are certain complicated functions of ϵ and θ given in (6.6) and (6.7). Also, the modified coordinates (λ, μ) of the airplane at the instant of missile release are given by (19.6) which read

$$\left.\begin{aligned} \lambda &= \rho \cos \epsilon - \frac{1}{n}[\sin \epsilon - \sin (\epsilon - \theta)], \\ \mu &= \rho \sin \epsilon + \frac{1}{n}[\cos \epsilon - \cos (\epsilon - \theta)]. \end{aligned}\right\} \tag{23.3}$$

To obtain the curve $Q = 0.1$ in Fig. 5, we first set $Q = 0.1$ and $\epsilon = 0°$ in (23.1) and compute the corresponding values of ρ. (This has already been done in Section 9.) Let us denote this value of ρ by $\bar{\rho}$. Equation (23.2) then yields the value of θ corresponding to $\rho = \bar{\rho}$, and $\epsilon = 0°$; we denote this value by $\bar{\theta}$. Equations (23.3) then yield the values of (λ, μ) corresponding to $\rho = \bar{\rho}$, $\epsilon = 0°$, and $\theta = \bar{\theta}$. The values of (λ, μ) then yield a point in the (λ, μ) plane of Fig. 5. It is the point corresponding to $Q = 0.1$ and $\epsilon = 0°$. In a similar fashion, we obtain points corresponding to $Q = 0.1$ and $\epsilon = 5°, 10°, 15°, \cdots, 45°$. A smooth curve is drawn through these 10 points; it is the curve $Q = 0.1$. By repeating the whole process, we obtain the curves $Q = 0.3, 0.5, 0.7, \cdots, 2.7$.

It will be noted that all the curves Q = const. are tangent to the envelope E; the point of tangency divides these curves into two parts, one of which appears in Fig. 5a and the other in Fig. 5b.

In the calculations described above it was necessary to compute from (23.2) values of θ corresponding to values of ρ and ϵ. A straightforward approach to this was impractical because of the complexity of the functions involved. Accordingly, this calculation was accomplished exactly as it was in Section 21, by the use of finite differences. The details of this process are contained in the last two paragraphs of Section 21.

SECTION 24: FIGURES 6-9

EXPLANATIONS

As mentioned in Section 1 and illustrated in Fig. 1, the airplane flies directly toward the target T with constant speed V along a straight line which makes an angle ϵ with the horizontal. When the airplane is at a distance R_o from the target, it pulls up in an ng turn, still maintaining a constant speed V. When the airplane has pulled up through an angle θ, a bomb is released which bursts at a point B, which is presumably near the target.

Let us refer to a set of values of ϵ, R_o, n, and θ which produce a burst on the target as <u>hit values</u>. Let us consider the case when the actual values of ϵ, R_o, n, and θ differ from hit values by small amounts, $\delta\epsilon$, δR, δn, and $\delta\theta$, respectively. These quantities, $\delta\epsilon$, δR, δn, and $\delta\theta$, represent errors and cause the burst to miss the target. Let δx_B denote the horizontal distance from the target to the point where the trajectory cuts the horizontal plane through the target, and let δy_B denote the vertical distance from the target to the point where the trajectory cuts the vertical line through the target; δx_B is positive and δy_B is negative when the trajectory passes on the near side of the target, while δy_B is positive and δx_B is negative when the trajectory passes on the far side of the target. Figure 10a illustrates the case when δx_B is positive, and Fig. 10b the case when δy_B is positive. In both cases, since the trajectory in the immediate neighborhood of the target may be regarded as a straight line, a knowledge of δx_B and δy_B permits us to construct the trajectory in this neighborhood; this is illustrated in Figs. 10a and 10b. If α is the angle which the trajectory makes with the horizontal plane through the target, as shown in Figs. 10a and 10b, then in both cases we have

$$\tan \alpha = - \delta y_B / \delta x_B. \qquad (24.1)$$

We now define E_x, E_y, E_θ, E_R, E_ϵ, and E_n by the relations

$$\left.\begin{aligned} E_x &= 100\,\frac{\delta x_B}{R_o}, \quad E_y = 100\,\frac{\delta y_B}{R_o}, \quad E_\theta = 100\,\frac{\delta\theta}{\theta}, \\ E_R &= 100\,\frac{\delta R_o}{R_o}, \quad E_\epsilon = 100\,\frac{\delta\epsilon}{\epsilon}, \quad E_n = 100\,\frac{\delta n}{n}. \end{aligned}\right\} \quad (24.2)$$

Thus, E_x is the percent that error δx_B is of the slant range R_o at pull-up beginning, and E_y has a similar meaning; also E_θ, E_R, E_ϵ, and E_n are the percent errors in θ, R, ϵ, and n, respectively.

It is proved in Section 26 that

$$E_x = \frac{E}{E_{x\theta}}, \quad E_y = \frac{E}{E_{y\theta}}, \quad (24.3)$$

where

$$E = E_\theta - \frac{1}{E_{\theta R}} E_R - \frac{1}{E_{\theta\epsilon}} E_\epsilon - \frac{1}{E_{\theta n}} E_n, \quad (24.4)$$

the quantities $E_{x\theta}$, $E_{y\theta}$, $E_{\theta R}$, $E_{\theta\epsilon}$, and $E_{\theta n}$ being certain error coefficients whose values may be obtained from Figs. 6-9 in a manner indicated below.

In Figs. 6 and 7 the modified range ρ is plotted horizontally and the pull-up angle θ is plotted vertically, as in Fig. 2. As explained in Section 4, to each pair of properly chosen values of (ρ, θ) there corresponds a bombing run and, thus, to each point in some region of the (ρ, θ) plane of Figs. 6 and 7 there corresponds a bombing run. In Fig. 6 there appear two families of curves labelled $E_{x\theta}$ = const. and $E_{y\theta}$ = const. These families of curves permit a determination of the values of the error coefficients $E_{x\theta}$ and $E_{y\theta}$ for any particular bombing run identified by the values of ρ, θ associated with it.

Similarly, there appear in Fig. 7 three families of curves labelled $E_{\theta R}$ = const., $E_{\theta\epsilon}$ = const., and $E_{\theta n}$ = const. These three families of curves permit also a determination of the values of the error coefficients $E_{\theta R}$, $E_{\theta\epsilon}$, and $E_{\theta n}$ for any particular bombing run identified by the values of ρ, θ associated with it.

In Figs. 8 and 9 the modified coordinates (λ, μ) of the airplane at pull-up beginning are plotted in the usual rectangular cartesian fashion, as in Fig. 4. As explained in Section 10, to each pair of properly chosen values of (λ, μ) there corresponds two bombing runs, one flatter than the other, the flatter one being referred to as being of S-type and the other one as being

of L-type. Thus, to each point in some region of the (λ, μ) plane of Figs. 8 and 9 there correspond two bombing runs, one of S-type and one of L-type. Those of S-type are referred to in Figs. 8a and 9a, while those of L-type are referred to in Figs. 8b and 9b. In Fig. 8 there appear two families of curves labelled $E_{x\theta}$ = const. and $E_{y\theta}$ = const., and in Fig. 9 three families of curves labelled $E_{\theta R}$ = const., $E_{\theta\epsilon}$ = const., and $E_{\theta n}$ = const. These five families of curves permit a determination of the values of the five error coefficients, $E_{x\theta}$, $E_{y\theta}$, $E_{\theta R}$, $E_{\theta\epsilon}$, and $E_{\theta n}$, for any particular bombing run identified by the values of (λ, μ) associated with it.

SECTION 25: FIGURES 6-9

EXAMPLES OF THEIR USE

Example 1.—Let us suppose an airplane approaches the target at 1000 ft/sec^{-1} with an angle of approach of 30° ($\pm$ 1°) and starts the pull-up at a range of 60,000 ft ($\pm$ 500 ft). The pull-up is into a turn of 3g ($\pm$ .1g). The pull-up angle is that indicated by Fig. 2 and has a maximum error of $\pm$ 1°. It is required to find the maximum values of the horizontal and vertical distances δx_B and δy_B from the target to the trajectory; these distances are illustrated in Fig. 10.

As in the previous examples, for convenience we take g = 32 ft/sec^{-2}. We have V = 1000, and the hit values are ϵ = 30°, R_o = 60,000, and n = 3. The standard length L' has the value $L' = V^2/g = 10^6/32 = 31{,}250$ ft. The hit value of ρ is then $\rho = R_o/L' = 1.92$, and the point A in Figs. 6 and 7 corresponds to the bombing run here which would produce a hit. From Fig. 6 it follows that the hit value of θ is 36.2°. It then follows from (24.2) that

$$\left.\begin{aligned} E_\theta &= \frac{100}{36.2}(\pm 1) = \pm 2.8, \quad E_R = \frac{100}{60{,}000}(\pm 500) = \pm .83, \\ E_\epsilon &= \frac{100}{30}(\pm 1) = \pm 3.3, \quad E_n = \frac{100}{3}(\pm .1) = \pm 3.3. \end{aligned}\right\} \tag{25.1}$$

From Figs. 6 and 7 it also follows by linear interpolation that

$$\left.\begin{aligned} E_{x\theta} &= -2.33, \quad E_{y\theta} = 1.76, \\ E_{\theta R} &= .83, \quad E_{\theta\epsilon} = 1.62, \quad E_{\theta n} = 4.67. \end{aligned}\right\} \tag{25.2}$$

Substitution in (24.4) from (25.1) and (25.2) then yields

$$E = (\pm 2.8) - \frac{1}{.83}(\pm .83) - \frac{1}{1.62}(\pm 3.3) - \frac{1}{4.67}(\pm 3.3).$$

In this equation the upper signs do not have to be chosen together, nor do the lower signs. The worst situations occur when the choice of signs makes every term on the right side have the same sign. When these worst situations occur, then E has the values

$$E = \pm\left[2.8 + \frac{.83}{.83} + \frac{3.3}{1.62} + \frac{3.3}{4.67}\right] = \pm 6.5. \qquad (25.3)$$

Substitution in (24.3) from (25.2) and (25.3) then yields

$$E_x = \frac{\pm 6.5}{-2.33} = \mp 2.8, \; E_y = \pm\frac{6.5}{1.76} = \pm 3.7. \qquad (25.4)$$

In (25.4) the upper signs go together, as do the lower signs. From (24.2) it now follows that

$$\delta x_B = \frac{E_x R_o}{100} = \frac{(\mp 2.8)(60{,}000)}{100} = \mp 1.6 \text{ x } 1000 \text{ ft},$$

$$\delta y_B = \frac{E_y R_o}{100} = \frac{(\pm 3.7)(60{,}000)}{100} = \pm 2.2 \text{ x } 1000 \text{ ft}.$$

In conclusion, then, the worst possible combination of errors produces trajectories which miss the target T by distances shown in Fig. 11.

Example 2.—Let us suppose an airplane is to approach a target at 1000 ft/sec^{-1} and is to begin the pull-up when the horizontal range is 60,000 ft and the altitude is 30,000 ft. This information is sufficient to specify two bombing runs, one of S-type and one of L-type. The identifying features of these two types are defined in Section 10, par. 2.

For each of the two bombing runs, there is a value of the angle of approach ϵ, the range R_o at pull-up beginning, and the pull-up angle θ. The values of ϵ and θ can be obtained from Fig. 4; the value of R_o follows from the given values of the horizontal range and the altitude so that

$$R_o = \sqrt{(60{,}000)^2 + (30{,}000)^2} = 67{,}082 \text{ ft}. \qquad (25.5)$$

Let us further suppose that the maximum error in ϵ is $\pm$ 1°, in R_o is $\pm$ 500 ft, in θ is $\pm$ 1°, and in the turn is $\pm$ 0.1 g. Let us find the maximum values of the horizontal and vertical distances δx_B and δy_B from the target to the trajectory.

As in the previous examples, we take $g = 32$ ft/sec^{-2}. We have $V = 1000$, so the standard length L' has the value $L' = V^2/g = 31{,}250$ ft. The modified coordinates of the airplane at pull-up beginning are thus

$$\left.\begin{aligned} \lambda &= \frac{x}{L'} = \frac{60{,}000}{31{,}250} = 1.920, \\ \mu &= \frac{y}{L'} = \frac{30{,}000}{31{,}250} = .960. \end{aligned}\right\} \qquad (25.6)$$

The point corresponding to these values of λ and μ is marked A in Fig. 4a and B in Fig. 4b. The points A and B refer to bombing runs of S-type and L-type, respectively. We shall consider these two bombing runs in turn.

Bombing Run of S-Type.—In this case the bomb travels a relatively flat trajectory. From Fig. 4a we obtain by linear interpolation the values $\epsilon = 26.6°$ and $\theta = 47.7°$. Of course, these are hit values, as are those in (25.5) and (25.6). From (24.2) it now follows that

$$\left.\begin{aligned} E_\theta &= \frac{100}{47.7}(\pm 1) = \pm 2.1, \quad E_R = \frac{100}{67{,}082}(\pm 500) = \pm .74, \\ E_\epsilon &= \frac{100}{26.6}(\pm 1) = \pm 3.8, \quad E_n = \frac{100}{3}(\pm 0.1) = \pm 3.3. \end{aligned}\right\} \qquad (25.7)$$

The point A, which identifies the bombing run under consideration, also appears in Figs. 8a and 9a. From these figures we obtain by linear interpolation the values

$$\left.\begin{aligned} E_{x\theta} &= -3.0, \quad E_{y\theta} = 2.0, \\ E_{\theta R} &= .55, \quad E_{\theta\epsilon} = -1.0, \quad E_{\theta n} = 2.6. \end{aligned}\right\} \qquad (25.8)$$

Substitution in (24.4) from (25.7) and (25.8) then yields

$$E_x = \frac{\pm 8.5}{-3.0} = \mp 2.8, \quad E_y = \frac{\pm 8.5}{2.0} = \pm 4.2. \qquad (25.10)$$

Of course, the upper signs in (25.10) go together, as do the lower signs. From (24.2) it now follows that

$$\delta x_B = \frac{E_x R_o}{100} = \frac{(\mp 2.8)(67{,}082)}{100} = \mp 1.9 \text{ x } 1000 \text{ ft},$$

$$\delta y_B = \frac{E_y R_o}{100} = \frac{(\pm 4.2)(67{,}082)}{100} = \pm 2.8 \text{ x } 1000 \text{ ft}.$$

The slope of the trajectory in the neighborhood of the target is $\delta y_B/\delta x_B = -1.5$.

Bombing Run of L-Type.—In this case the bomb travels a relatively steep trajectory. From Fig. 4b we obtain by linear interpolation the values $\epsilon = 26.6°$ and $\theta = 78.3°$; from (24.2) it follows that

$$\left.\begin{aligned} E_\theta &= \frac{100}{78.3}(\pm 1) = \pm 1.3, \quad E_R = \frac{100}{67{,}082}(\pm 500) = \pm .74, \\ E_\epsilon &= \frac{100}{26.6}(\pm 1) = \pm 3.8, \quad E_n = \frac{100}{3}(\pm 0.1) = \pm 3.3. \end{aligned}\right\} \qquad (25.11)$$

The point B, which in Fig. 4b identifies the bombing run under consideration, also appears in Figs. 8b and 9b. From these figures we obtain for this point by linear interpolation the values

$$\left.\begin{aligned} E_{x\theta} &= 2.1, \quad E_{y\theta} = -.55, \\ E_{\theta R} &= -.93, \quad E_{\theta\epsilon} = 1.1, \quad E_{\theta n} = -3.1. \end{aligned}\right\} \qquad (25.12)$$

Substitution in (24.4) from (25.11) and (25.12) then yields

$$E = (\pm 1.3) - \frac{1}{-.93}(\pm .74) - \frac{1}{1.1}(\pm 3.8) - \frac{1}{-3.1}(\pm 3.3).$$

As before, when the worst situations arise, we have

$$E = \pm\left[1.3 + \frac{.74}{.93} + \frac{3.8}{1.1} + \frac{3.3}{3.1}\right] = \pm 6.7. \qquad (25.13)$$

Substitution in (24.3) from (25.12) and (25.13) then yields

$$E_x = \frac{\pm 6.7}{2.1} = \pm 3.2, \; E_y = \frac{\pm 6.7}{-.55} = \mp 12. \qquad (25.14)$$

From (24.2) it now follows that

$$\delta x_B = \frac{E_x R_o}{100} = \frac{(\pm 3.2)(67{,}082)}{100} = \pm 2.1 \times 1000 \text{ ft},$$

$$\delta y_B = \frac{E_y R_o}{100} = \frac{(\mp 12)(67{,}082)}{100} = \mp 8.0 \times 1000 \text{ ft}.$$

The slope of the trajectory in the neighborhood of the target is $\delta y_B/\delta x_B = -3.8$, which is much larger in absolute value than in the case of the bombing run of S-type considered just above, as is to be expected.

SECTION 26: FIGURES 6-9

THEORY

The basic equation is (6.1) which is

$$\rho^2 - 2\Phi\rho + \Psi = 0, \qquad (26.1)$$

where

$$\Phi = \frac{1}{2(\xi_B - \cos\epsilon)}\left\{\sin 2(\epsilon - \theta) - \frac{\zeta_B - \sin\epsilon}{\xi_B - \cos\epsilon}[1 + \cos 2(\epsilon - \theta)] - \frac{2}{n}[\sin\epsilon - \sin(\epsilon - \theta)]\right\}, \qquad (26.2)$$

$$\Psi = \frac{1}{n(\xi_B - \cos\epsilon)^2}\left\{2(1-\cos\theta)\cos(\epsilon-\theta) + \frac{1}{n}[\sin\epsilon - \sin(\epsilon-\theta)]^2\right\}. \tag{26.3}$$

Here, ρ is modified range at pull-up beginning, ϵ is the angle of approach, θ is the pull-up angle, n is the pull-up constant, and (ξ_B, ζ_B) are the modified coordinates of the burst. We can write (26.1) in the form

$$f(\xi_B, \zeta_B, \theta, \rho, \epsilon, n) = 0. \tag{26.4}$$

As mentioned earlier, when the bomb bursts on the target, then $\xi_B = \zeta_B = 0$ and the values of ρ, θ, ϵ, and n are called hit values. Such values satisfy the equation

$$f(0, 0, \theta, \rho, \epsilon, n) = 0. \tag{26.5}$$

Let $\delta\xi_B$, $\delta\zeta_B$, $\delta\theta$, $\delta\rho$, $\delta\epsilon$, and δn denote small changes in the variables. Then (26.4) yields

$$f_\xi\,\delta\xi_B + f_\zeta\,\delta\zeta_B + f_\theta\,\delta\theta + f_\rho\,\delta\rho + f_\epsilon\,\delta\epsilon + f_n\,\delta n = 0, \tag{26.6}$$

where

$$\left.\begin{aligned} f_\xi &= \frac{\partial f}{\partial \xi_B}, \quad f_\zeta = \frac{\partial f}{\partial \zeta_B}, \quad f_\theta = \frac{\partial f}{\partial \theta}, \\ f_\rho &= \frac{\partial f}{\partial \rho}, \quad f_\epsilon = \frac{\partial f}{\partial \epsilon}, \text{ and } f_n = \frac{\partial f}{\partial n}. \end{aligned}\right\} \tag{26.7}$$

In (26.6) we shall evaluate the partial derivatives for hit values of the variables; it then follows that $\delta\xi_B$, $\delta\zeta_B$, $\delta\theta$, $\delta\rho$, $\delta\epsilon$, and δn are amounts by which the actual values of the variables differ from hit values and, hence, (26.6) permits a determination of the amounts by which the burst misses the target, both in horizontal range and elevation, due to small errors in θ, ρ, ϵ, and n. This determination will now be made and the result expressed in terms of the unmodified variables x_B, y_B, θ, R_o, ϵ, and n rather than the modified variables. For this purpose we make the following definitions:

$$\left.\begin{aligned}
&\text{Percent that } \delta x_B \text{ is of } R_o = 100\,\frac{\delta x_B}{R_o} = E_x,\\
&\text{Percent that } \delta y_B \text{ is of } R_o = 100\,\frac{\delta y_B}{y_B} = E_y,\\
&\text{Percent change in } \theta = 100\,\frac{\delta\theta}{\theta} = E_\theta,\\
&\text{Percent change } R_o = 100\,\frac{\delta R_o}{R_o} = E_R,\\
&\text{Percent change in } \epsilon = 100\,\frac{\delta\epsilon}{\epsilon} = E_\epsilon,\\
&\text{Percent change in } n = 100\,\frac{\delta n}{n} = E_n;
\end{aligned}\right\} \qquad (26.8)$$

$$\left.\begin{aligned}
E_{x\theta} &= \text{percent change in } \theta \text{ which alone makes } E_x = 1,\\
E_{y\theta} &= \text{percent change in } \theta \text{ which alone makes } E_y = 1,\\
E_{\theta R} &= \text{percent change in } R_o \text{ which alone makes } E_\theta = 1,\\
E_{\theta\epsilon} &= \text{percent change in } \epsilon \text{ which alone makes } E_\theta = 1,\\
E_{\theta n} &= \text{percent change in } n \text{ which alone makes } E_\theta = 1.
\end{aligned}\right\} \qquad (26.9)$$

In (26.4) the variables (ξ_B, ζ_B) may be regarded as the modified coordinates of a general point on the trajectory of the bomb. We shall consider in turn the point where the trajectory pierces the horizontal plane through the target and the point where the trajectory cuts the vertical line through the target.

The Point Where the Trajectory Cuts the Horizontal Plane Through the Target.—For this point $\delta\zeta_B = 0$ and (26.6) yields

$$\delta\xi_B = -\frac{1}{f_\xi}\left[f_\theta\,\delta\theta + f_\rho\,\delta\rho + f_\epsilon\,\delta\epsilon + f_n\,\delta n\right]. \qquad (26.10)$$

Now $x_B = R_o\,\xi_B$, and so

$$\delta x_B = R_o\,\delta\xi_B + \xi_B\,\delta R_o.$$

Since all coefficients are evaluated for hit values of the variables, this equation reduces to $\delta x_B = R_o \, \delta\xi_B$, whence it follows from (26.8) that

$$100 \, \delta\xi_B = 100 \, \frac{\delta x_B}{R_o} = E_x. \tag{26.11}$$

Also, $L' \rho = R_o$, where L' is a standard length introduced in Section 3. Hence,

$$\frac{\delta\rho}{\rho} = \frac{\delta R_o}{R_o},$$

and from (26.8) it then follows that

$$100 \, \frac{\delta\rho}{\rho} = 100 \, \frac{\delta R_o}{R_o} = E_R. \tag{26.12}$$

We now substitute in (26.10) for $\delta\xi_B$ and $\delta\rho$ from (26.11) and (26.12) and for $\delta\theta$, $\delta\epsilon$, and δn from (26.8) to obtain

$$E_x = - \frac{1}{f_\xi} [\theta f_\theta E_\theta + \rho f_\rho E_R + \epsilon f_\epsilon E_\epsilon + n f_n E_n]. \tag{26.13}$$

Let us now refer to the symbols defined in (26.9). We note that $E_x = 1$ when $E_\theta = E_{n\theta}$ and $E_R = E_\epsilon = E_n = 0$. Hence, (26.13) yields

$$1 = - \frac{\theta f_\theta}{f_\xi} E_{x\theta} \text{ or } - \frac{\theta f_\theta}{f_\xi} = \frac{1}{E_{x\theta}}. \tag{26.14}$$

Similarly, we have

$$\left.\begin{aligned} \theta f_\theta + \rho f_\rho E_{\theta R} &= 0, \\ \theta f_\theta + \epsilon f_\epsilon E_{\theta\epsilon} &= 0, \\ \theta f_\theta + n f_n E_{\theta n} &= 0. \end{aligned}\right\} \tag{26.15}$$

Substitution in (26.13) for f_ρ, f_ϵ, and f_n from (26.15) then yields

$$E_x = -\frac{\theta f_\theta}{f_\xi}\left[E_\theta - \frac{1}{E_{\theta R}}E_R - \frac{1}{E_{\theta\epsilon}}E_\epsilon - \frac{1}{E_{\theta n}}E_n\right].$$

Because of (26.14), this equation becomes

$$E_x = E/E_{x\theta}, \tag{26.16}$$

where

$$E = E_\theta - \frac{1}{E_{\theta R}}E_R - \frac{1}{E_{\theta\epsilon}}E_\epsilon - \frac{1}{E_{\theta n}}E_n. \tag{26.17}$$

The Point Where the Trajectory Cuts the Vertical Line Through the Target.—For this point we have $\delta\xi_B = 0$, and so (26.6) yields

$$\delta\zeta_B = -\frac{1}{f_\zeta}[f_\theta\,\delta\theta + f_\rho\,\delta\rho + f_\epsilon\,\delta\epsilon + f_n\,\delta n]. \tag{26.18}$$

By proceeding as in the previous case, we find that

$$100\,\delta\zeta_B = E_y, \quad -\frac{\theta f_\theta}{f_\zeta} = \frac{1}{E_{y\theta}} \tag{26.19}$$

and that (26.18) ultimately becomes

$$E_y = E/E_{y\theta} \tag{26.20}$$

where E is as defined in (26.17).

With the establishment of (26.16) and (26.20) we have completed the derivation of Equations (24.3) which are basic in the error theory under consideration here.

There still remains the determination of expressions from which the coefficients $E_{x\theta}$, $E_{y\theta}$, $E_{\theta R}$, $E_{\theta\epsilon}$, and $E_{\theta n}$ can be readily computed. From (26.14), (26.15), and (26.19) we have the relations

$$\left.\begin{aligned} E_{x\theta} &= -\frac{f_\xi}{\theta\, f_\theta}, \quad E_{y\theta} = -\frac{f_\zeta}{\theta\, f_\theta}, \\ E_{\theta R} &= -\frac{\theta\, f_\theta}{\rho\, f_\rho}, \quad E_{\theta\epsilon} = -\frac{\theta\, f_\theta}{\epsilon\, f_\epsilon}, \quad E_{\theta n} = -\frac{\theta\, f_\theta}{n\, f_n}. \end{aligned}\right\} \tag{26.21}$$

Now $f = \rho^2 - 2\Phi\rho + \Psi$, where Φ and Ψ are defined in (26.2) and (26.3). The various expressions in (26.21) which involve f denote partial derivatives and and are defined precisely in (26.7). Of course, these partial derivatives are to be evaluated for hit values of the variables, that is, when $\xi_B = \zeta_B = 0$. A straightforward but lengthy calculation of these derivatives yields the expressions

$$\left.\begin{aligned} E_{x\theta} &= -\frac{A\rho - B}{\theta(D\rho - F)}, \quad E_{y\theta} = -\frac{C\rho}{\theta(D\rho - F)}, \\ E_{\theta R} &= \frac{\theta(D\rho - F)}{\rho(\rho - \Phi)\cos^2\epsilon}, \quad E_{\theta\epsilon} = -\frac{\theta(D\rho - F)}{\epsilon(G\rho - H)}, \\ E_{\theta n} &= -\frac{\theta(D\rho - F)}{n(I\rho - J)}, \end{aligned}\right\} \tag{26.22}$$

where

$$A = \Phi\cos\epsilon + \frac{1}{2}\tan\epsilon\,[1 + \cos 2(\epsilon - \theta)],$$

$$B = \Psi\cos\epsilon,$$

$$C = -\frac{1}{2}[1 + \cos 2(\epsilon - \theta)],$$

$$D = \cos(\epsilon - 2\theta) + \frac{1}{n}\cos\epsilon\cos(\epsilon - \theta),$$

$$F = \frac{1}{n}[\sin(\epsilon - \theta) - \sin(\epsilon - 2\theta)] + \frac{1}{n^2}[\sin\epsilon - \sin(\epsilon - \theta)]\cos(\epsilon - \theta),$$

$$G = \frac{1}{2}\left[\Phi\sin 2\epsilon + \frac{1 + \cos 2(\epsilon - \theta)}{\cos\epsilon}\right] - \cos(\epsilon - 2\theta) + \frac{\cos\epsilon}{n}[\cos\epsilon - \cos(\epsilon - \theta)],$$

$$H = \frac{1}{2}\Psi\sin 2\epsilon - \frac{1}{n}(1 - \cos\theta)\sin(\epsilon - \theta) + \frac{1}{n^2}[\sin\epsilon - \sin(\epsilon - \theta)][\cos\epsilon - \cos(\epsilon - \theta)],$$

$$I = -\frac{\cos\epsilon}{n^2}[\sin\epsilon - \sin(\epsilon - \theta)],$$

$$J = -\Psi\frac{1 + \cos 2\epsilon}{4n} - \frac{1}{2n^3}[\sin\epsilon - \sin(\epsilon - \theta)]^2.$$

The actual determination of the curve families in Figs. 6-9 is as follows. The first step is the tabulation of the values of A, B, C, D, F, G, H, I, and J for $\epsilon = 0°, 10°, 20°, 30°, 40°$, and $45°$ and for $\theta = 0°, 5°, 10°, \cdots, 90° + \epsilon$. In this regard, the quantities Φ and Ψ appearing in the expressions above are given by (26.2) and (26.3) with $\xi_B = \zeta_B = 0$ and were tabulated for the above values of ϵ and θ in a calculation referred to in Section 6. The second step is the utilization of the results of the first step and of Equations (26.22) to tabulate the values of the error coefficients $E_{x\theta}$, $E_{y\theta}$, $E_{\theta R}$, $E_{\theta\epsilon}$, and $E_{\theta n}$ for $\epsilon = 0°, 10°, 20°, 30°, 40°$, and $45°$ and $\theta = 0°, 5°, 10°, \cdots, 90° + \epsilon$.

The third step first requires the determination of values of ϵ and θ corresponding to various assigned values of the error coefficients. Finite-difference methods were tried extensively here but were abandoned due to lack of flexibility and to the extent of the labor involved. Graphical methods were used instead. The procedure in the case of Fig. 6 is as follows. The coefficient $E_{x\theta}$ is plotted against θ for $\epsilon = 0$, and from this graph the values of θ are obtained corresponding to $E_{x\theta} = -1.5, -2, -2.5, -3, -4, -5, -10, \mp\infty, 10, 3, 1, .5, .25$, and 0. On Fig. 6, where ρ is plotted horizontally and θ is plotted vertically, the curve $\epsilon = 0°$ is drawn; it is taken directly from Fig. 2. On this curve there are located points corresponding to the values of θ determined as above. Similar procedures are carried out for $\epsilon = 10°, 20°, 30°, 40°$, and $45°$. We thus obtain a sequence of points corresponding to $E_{x\theta} = -1.5$, a second sequence corresponding to $E_{x\theta} = -2$, and so on. Through each sequence a smooth curve is drawn. The family of curves thus obtained is the family $E_{x\theta} = \text{const.}$ in Fig. 6. A similar procedure yields the family $E_{y\theta} = \text{const.}$ in Fig. 6 and the families $E_{\theta R}$, $E_{\theta\epsilon}$, and $E_{\theta n}$ in Fig. 7. In Fig. 6 the curve $E_{x\theta} = \infty$ is just the curve $\rho = \rho_{max}$ of Fig. 2; this curve is also the curve $E_{y\theta} = \infty$ in Fig. 6 and the curve $E_{\theta R} = E_{\theta\epsilon} = E_{\theta n} = 0$ in Fig. 7. Also, in Fig. 6 the curve $E_{x\theta} = 0$ is the curve corresponding to bombing runs in which the airplane releases the bomb vertically upward from a point vertically above the target. This curve is also the curve $E_{y\theta} = 0$ in Fig. 6, and the curves $E_{\theta R} = -\infty$, $E_{\theta\epsilon} = \infty$, and $E_{\theta n} = -\infty$ in Fig. 7.

The procedure for the actual determination of the curve families in Figs. 8 and 9 is as follows. About halfway through the preceding paragraph it was explained how there was obtained on the curve $\epsilon = 0°$ in Fig. 6 a set of points corresponding to certain constant values of $E_{x\theta}$. From Fig. 6 the values of ρ corresponding to these points are read off and the values of λ computed by use of the relation $\lambda = \rho\cos\epsilon$. We have thus a set of values of

λ corresponding to $\epsilon = 0°$ and $E_{x\theta} = -1.5, -2, -2.5, -3, -4, -5, -10, \mp\infty, 10, 3, 1, .5, .25$, and 0. On Fig. 8, where λ is plotted horizontally, the curve $\epsilon = 0°$ is drawn; it is taken directly from Fig. 4. On this curve there are located points corresponding to the values of λ just determined. Similar procedures are carried out for $\epsilon = 10°, 20°, 30°, 40°$, and $45°$. We thus obtain a sequence of points corresponding to $E_{x\theta} = -1.5$, a second sequence corresponding to $E_{x\theta} = -2$, and so on. Through each sequence a smooth curve is drawn. The family of curves thus obtained is the family $E_{x\theta} =$ const. in Fig. 8. Actually, this family of curves has an envelope which is just the curve $\rho = \rho_{max}$. The point where each member of the family touches the envelope divides the curve into two parts; one part corresponds to bombing runs of S-type (flat trajectories), while the other yields bombing runs of L-type (steep trajectories). To avoid confusion, the part of the family corresponding to bombing runs of S-type appears in Fig. 8a, while the part of the family corresponding to bombing runs of L-type appears in Fig. 8b. A similar procedure yields the curves $E_{y\theta} =$ const. in Figs. 8a, and 8b and the curves $E_{\theta R} =$ const., $E_{\theta\epsilon} =$ const., and $E_{\theta n} =$ const. in Figs. 9a and 9b.

SECTION 27: FIGURES 12-14

EXPLANATIONS AND THEORY

These figures show typical bombing runs. In Fig. 12 the angle of approach ϵ has the value 0°, and the pull-up angle θ has the values 30° and 60°; similarly, in Fig. 13, $\epsilon = 20°$ and $\theta = 30°, 60°$, and $90°$; in Fig. 14, $\epsilon = 40°$ and $\theta = 30°, 60°, 90°$, and $120°$.

In the construction of these graphs only the determination of the parabolic arcs offers any difficulty. If (x, y) are the coordinates of a general point on the parabolic arc, then the equation of this arc has the form

$$4a(y - k) = -(x - h)^2, \qquad (27.1)$$

where (h, k) are the coordinates of the vertex of the parabolic arc and 4a is the length of its latus rectum. A knowledge of h, k, and a permits a rapid construction of the parabolic arc.

We first introduce the dimensionless length $\underline{L}'$ defined in Section 3 and also introduce the dimensionless quantities λ, μ, $\underline{a}$, $\underline{h}$, and $\underline{k}$ defined by the relations

$$\left.\begin{aligned} \lambda &= x/L', \ \mu = y/L', \\ \bar{a} &= a/L', \ \bar{h} = h/L', \ \bar{k} = k/L'. \end{aligned}\right\} \tag{27.2}$$

Then Equation (27.1) takes the form

$$4\bar{a}(\bar{k} - \mu) = (\lambda - \bar{h})^2. \tag{27.3}$$

Let us refer to Fig. 1. The locus of Equation (27.3) must pass through the origin T of the coordinates and through the point R with modified coordinates (λ_R, μ_R). Also at R, this locus must have the slope $\tan(\epsilon - \theta)$. These three conditions yield three equations

$$4\bar{a}\,\bar{k} = \bar{h}^2, \ -4\bar{a}\mu_R = \lambda_R^2 - 2\bar{h}\lambda_R, \ -4\bar{a}\tan(\epsilon - \theta) = 2(\lambda_r - \bar{h}).$$

We solve these equations for $\bar{a}$, $\bar{h}$, and $\bar{k}$, obtaining the results

$$\left.\begin{aligned} \bar{a} &= \frac{\lambda_R}{4[\tan\gamma - \tan(\epsilon - \theta)]}, \\ \bar{h} &= 2\bar{a}[2\tan\gamma - \tan(\epsilon - \theta)], \\ \bar{k} &= \frac{1}{2}\bar{h}[2\tan\gamma - \tan(\epsilon - \theta)], \end{aligned}\right\} \tag{27.4}$$

where $\tan\gamma = \mu_R/\lambda_R$. Equations (27.4) permit a simple computation of values of a, h, and k; this in turn permits a rapid construction of the parabolic arcs in Figs. 12-14.

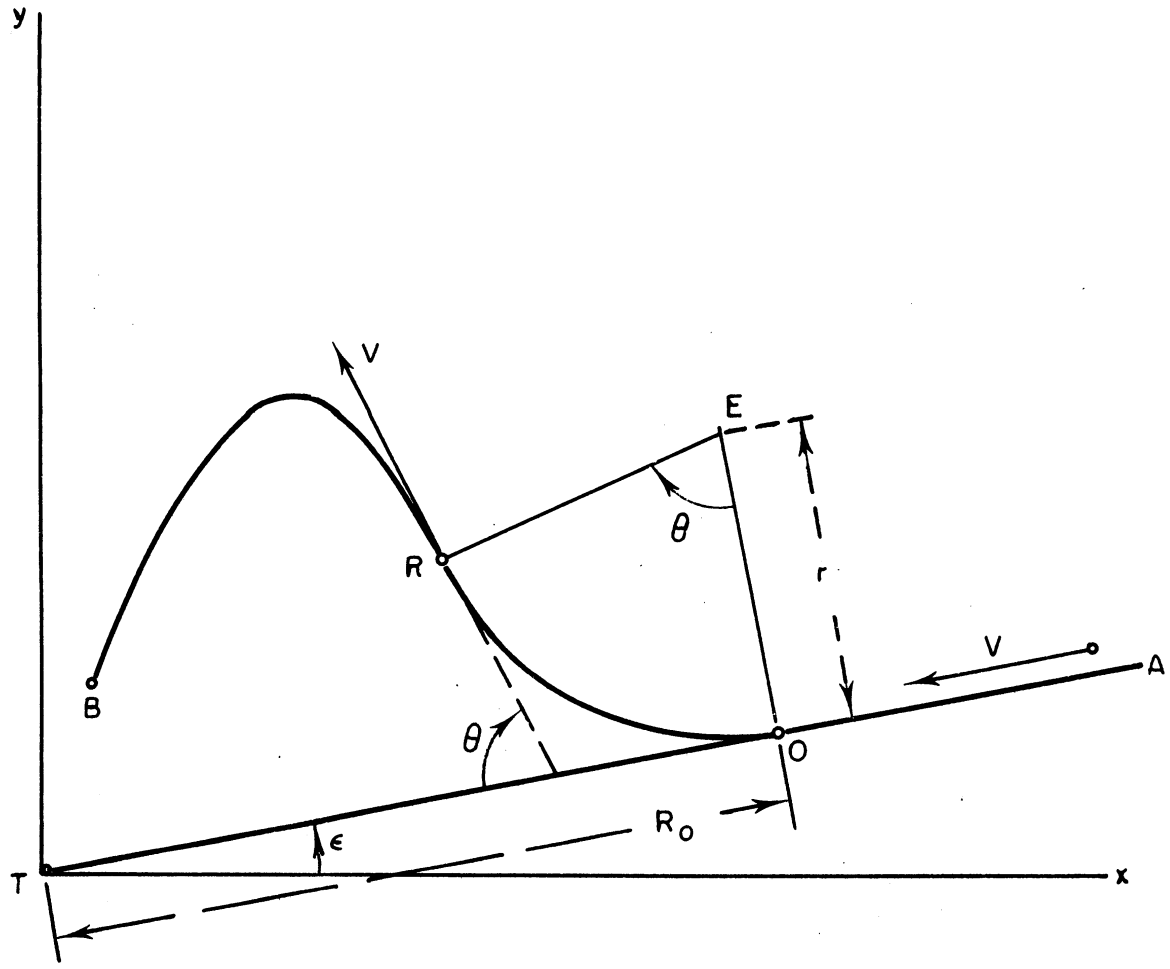

Fig. 1. A general bombing run.

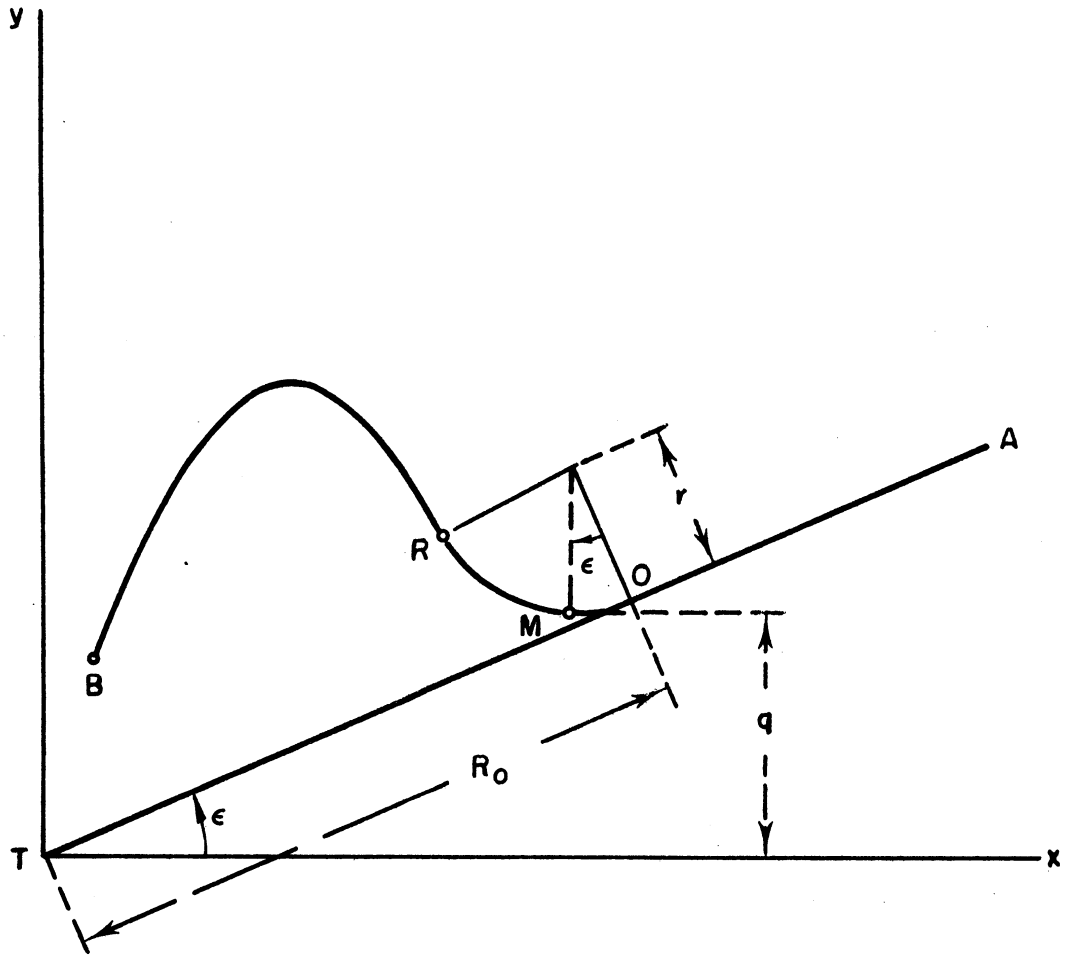

Fig. 3. A general bombing run.

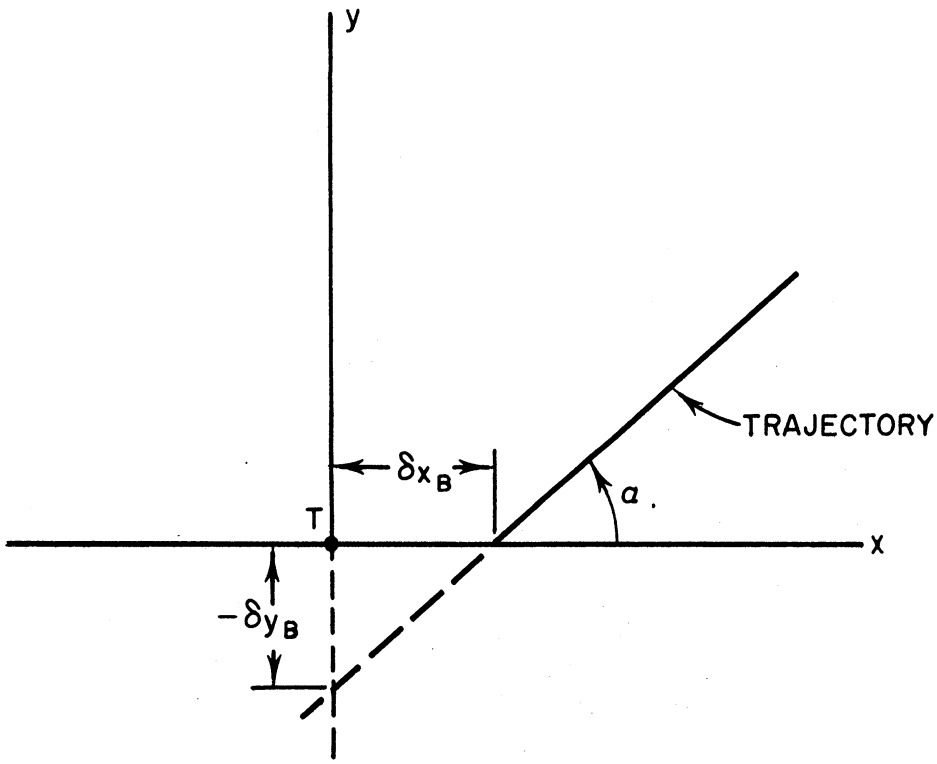

Fig. 10a. A part near the target T of the trajectory when there is undershooting.

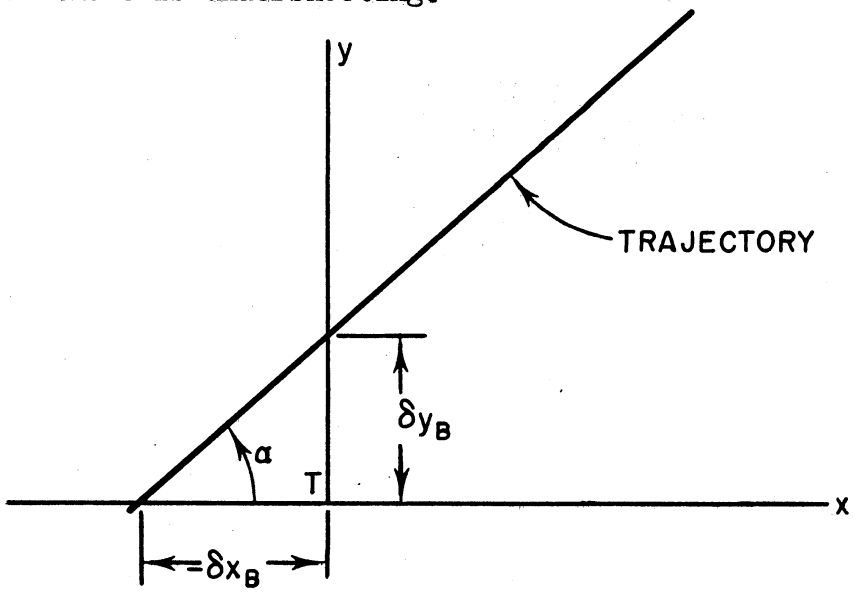

Fig. 10b. A part near the target T of the trajectory when there is overshooting.

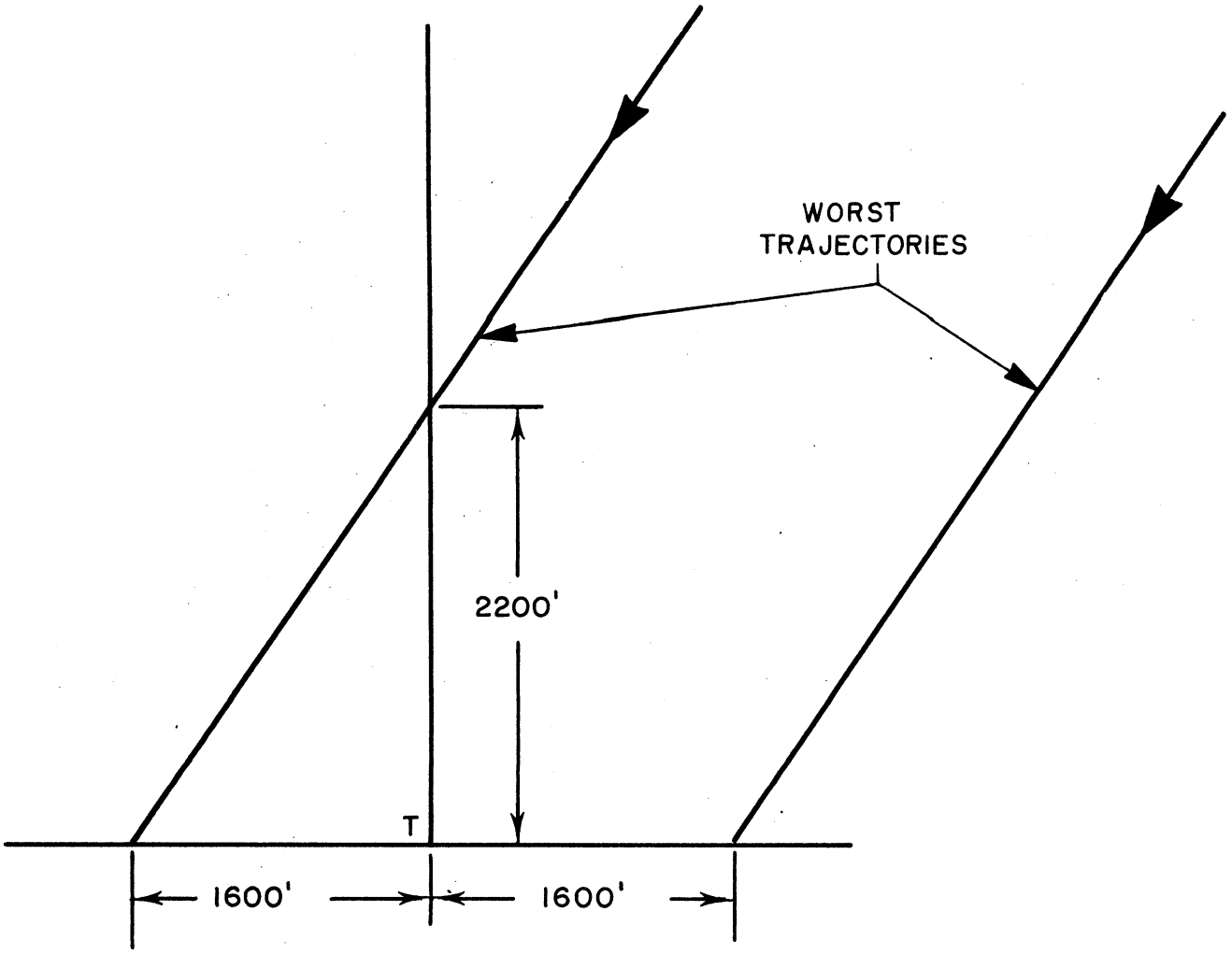

Fig. 11. A part near the target T of the two worst trajectories of Example 1 of Section 25.

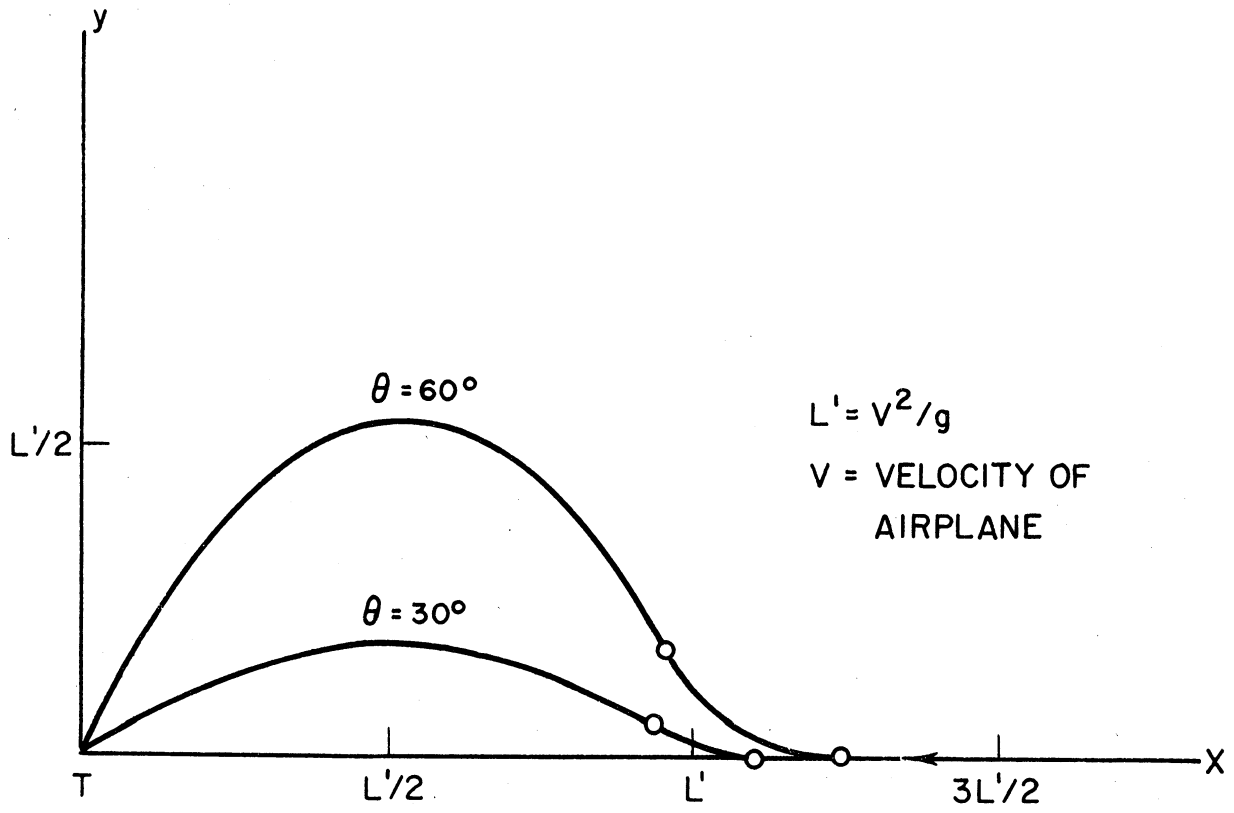

Fig. 12. Bombing runs for $\epsilon = 0°$ and $\theta = 30°$ and $60°$.

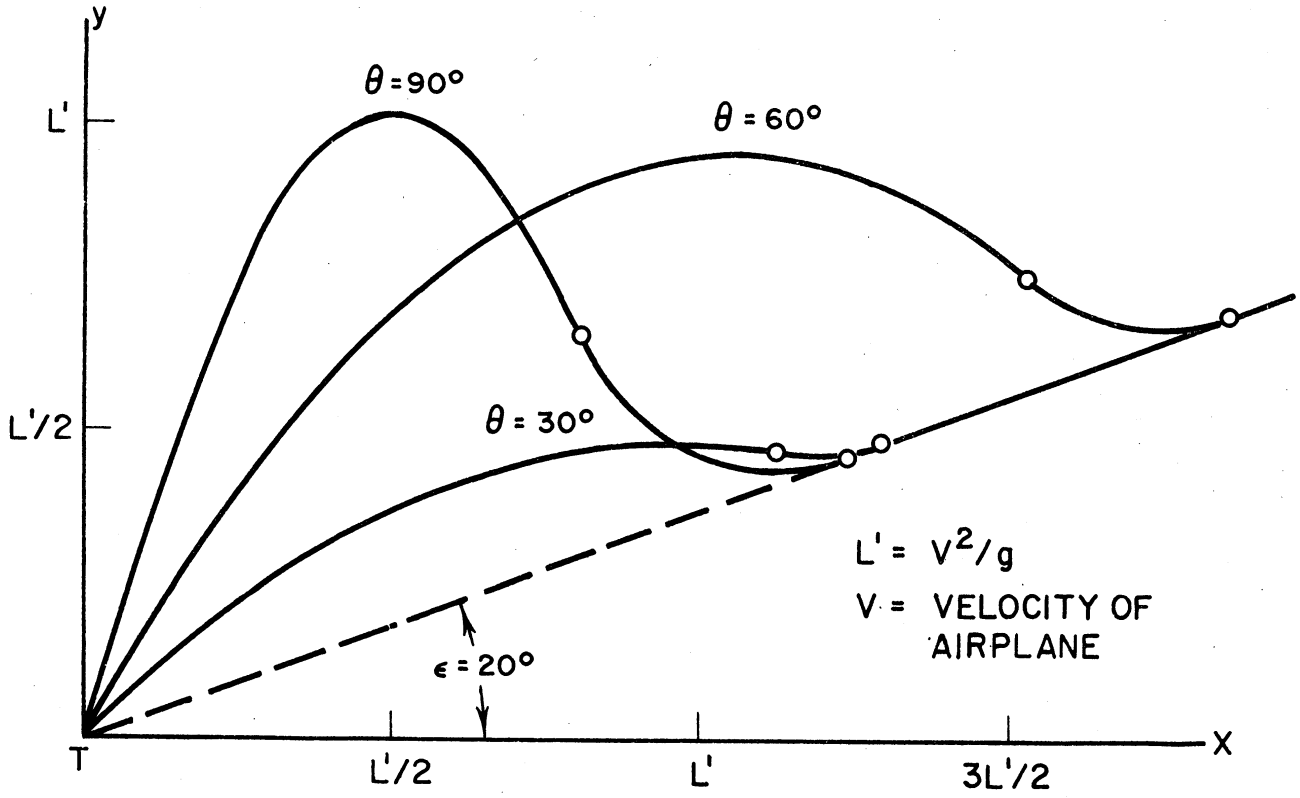

Fig. 13. Bombing runs for $\epsilon = 20°$ and $\theta = 30°$, $60°$, and $90°$.

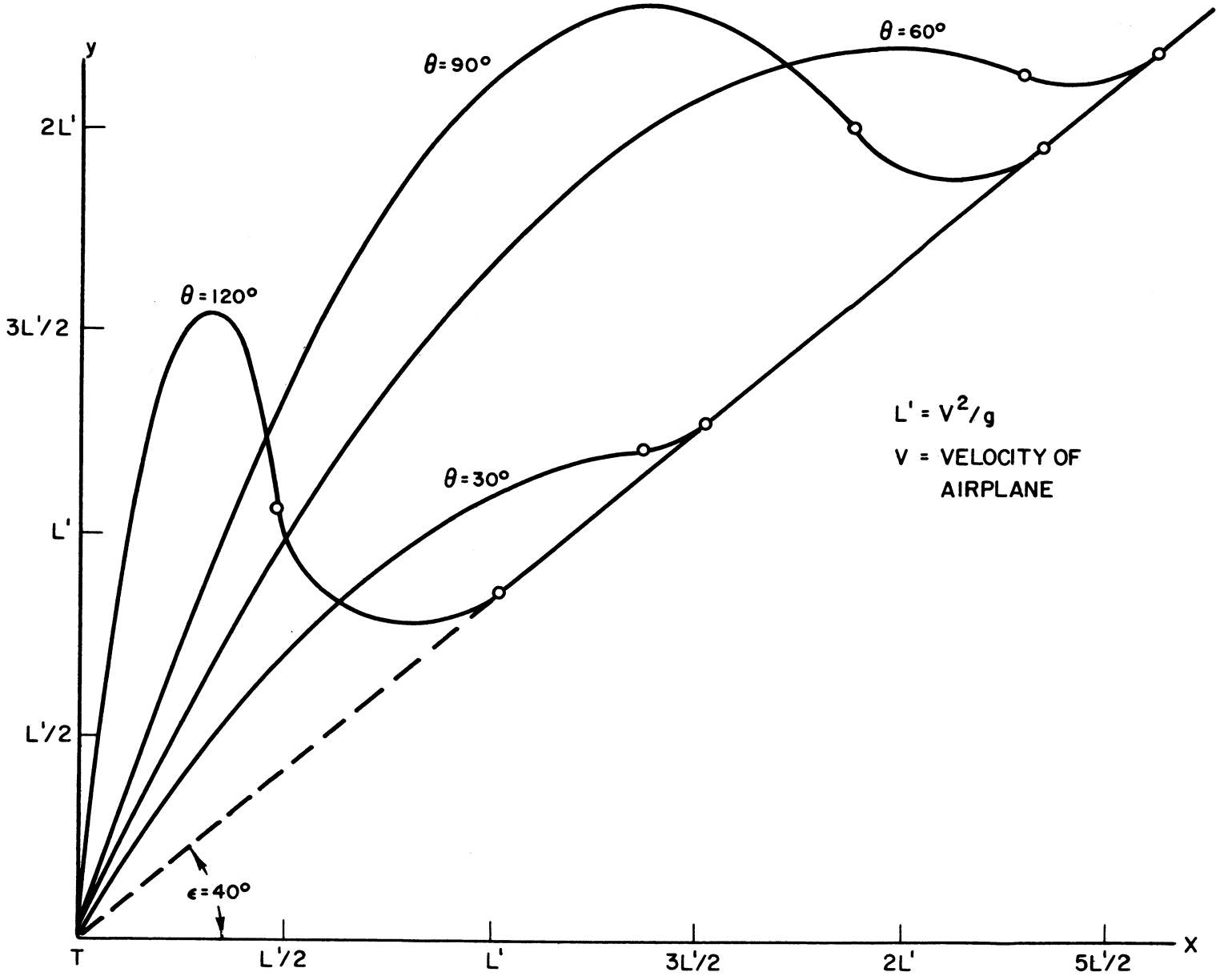

Fig. 14. Bombing runs for $\epsilon = 0°$ and for $\theta = 30°$, $60°$, $90°$, and $120°$.